SYNTHESIS OF MINERALS (NANO-) AND NANOPARTICLES FOR RESEARCH AND APPLICATIONS

CONTACT: GERMAN MONTES HERNANDEZ

german.montes-hernandez@univ-grenoble-alpes.fr

CATALOG

- ALL MINERALS AND PARTICLES ARE SYNTHESIZED USING IN-HOUSE METHODS AND PROTOCOLS.
- MILD AND HYDROTHERMAL CONDITIONS ARE GENERALLY USED
- CALCINATION IS SOMETIME ALSO USED
- AMOUNT FROM 5 TO 100G

- FOR BASIC AND/OR APPLIED RESEARCH
- VIA RESEARCH COLLABORATIONS
- VIA ACADEMIC CONTRACTS
- VIA EXTERNAL SERVICE

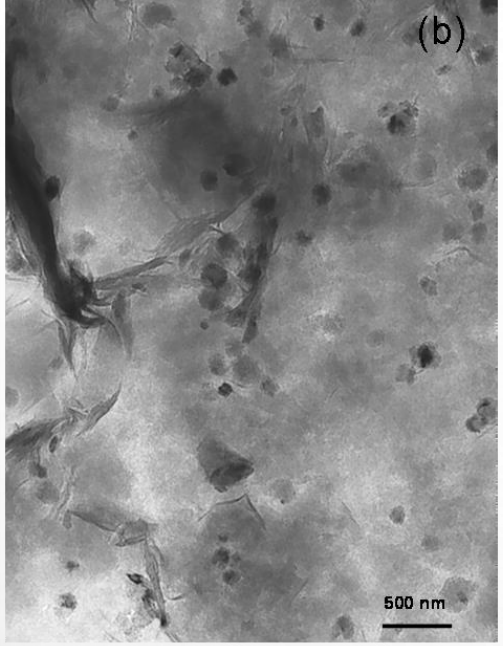

Fe_2O_3 on clay

Smectite-Hematite red composite from clay alteration in presence of iron and carbon dioxide

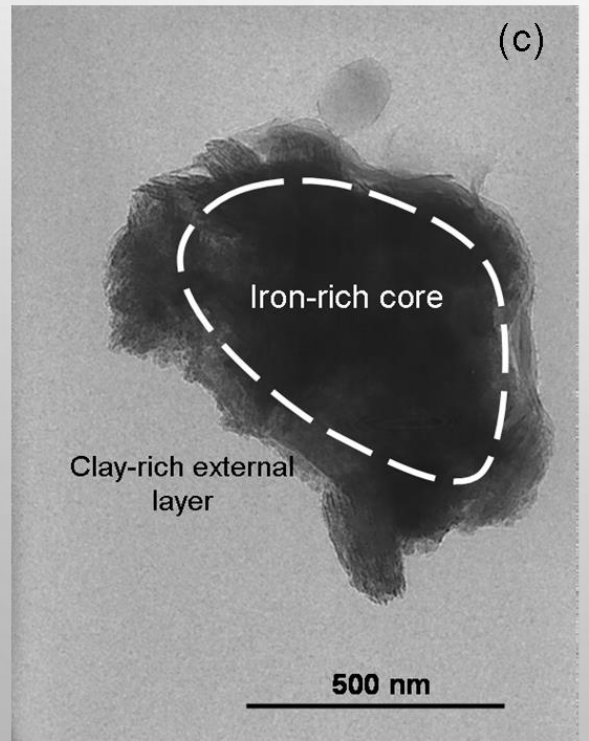

- G. Montes-Hernandez, J. Pironon, Hematite and iron carbonate precipitation-coexistence at the iron-montmorillonite-salt solution-CO2 interfaces under high gas pressure at 150 C. Applied Clay Science 45 (2009) 194-200.

- G. Montes-Hernandez, J. Pironon, F. Villieras, Synthesis of a red iron oxide/montmorillonite pigment in a CO2-rich brine solution. Journal of Colloid and Interface Science 303 (2006) 472-476.

$CaCO_3$

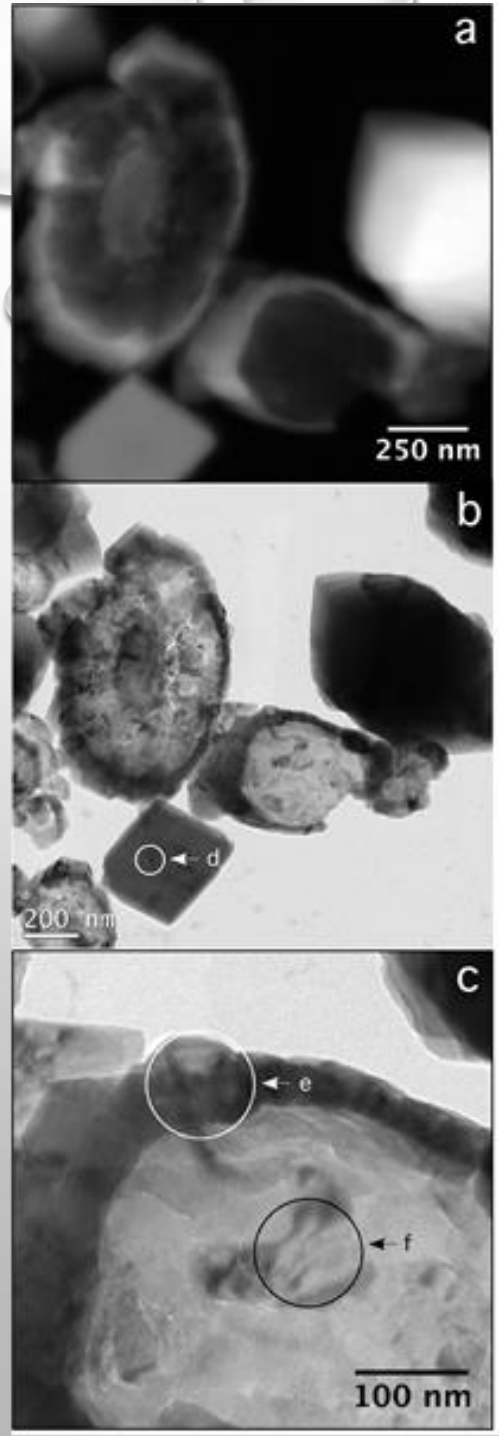

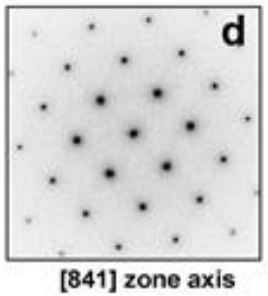

[841] zone axis

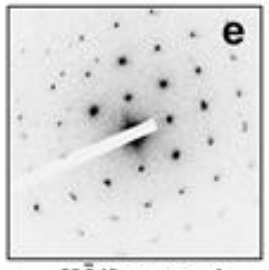

[2$\bar{2}$1] zone axis

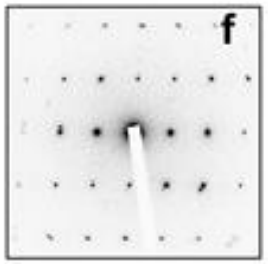

[271] zone axis

Nano-structured calcite precipitated in presence of selenium compounds

- G. Montes-Hernandez, G. Sarret, R. Hellmann, N. Menguy, D. Testemale, L. Charlet, F. Renard. Nanostructured calcite precipitated under hydrothermal conditions in the presence of organic and inorganic selenium. Chemical Geology 290 (2011) 109-120.

SeNPs-Calcite composite by oxidative fragmentation of selenocystine during portlandite carbonation

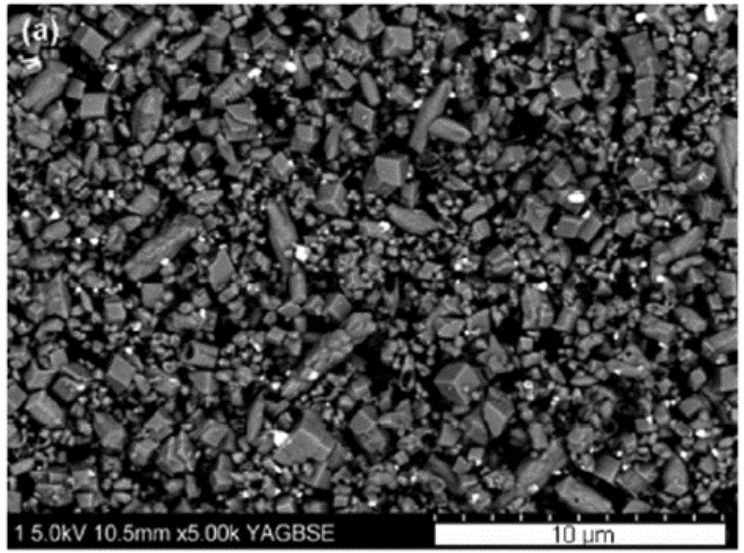

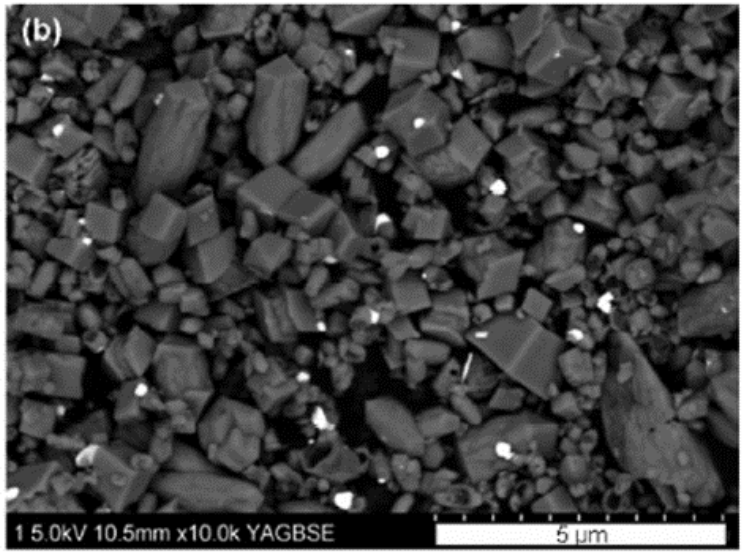

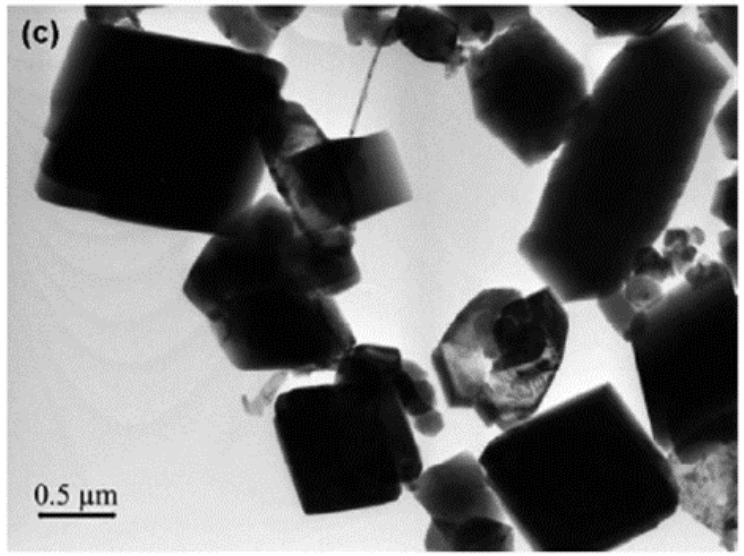

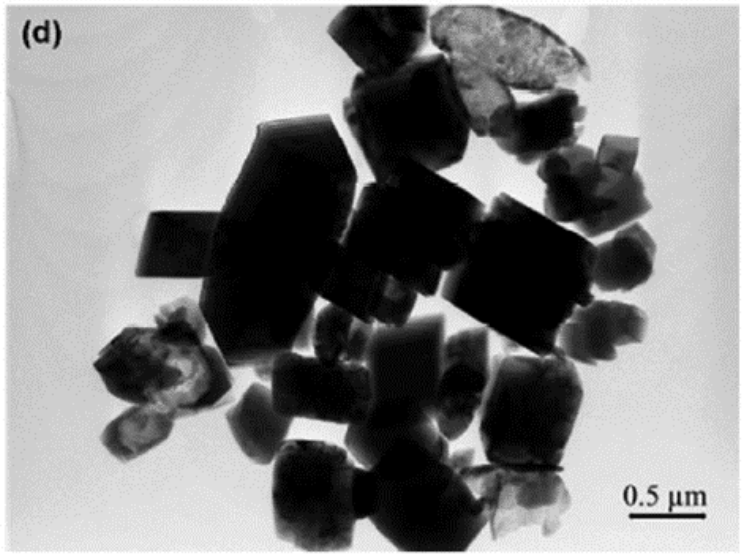

Se^0-$CaCO_3$

- G. Montes-Hernandez, A. Fernandez-Martinez, L. Charlet, F. Renard, A. Scheinost, M. Bueno, Synthesis of a Se0/calcite composite using hydrothermal carbonation of Ca(OH)2 coupled to a complex selenocystine fragmentation. Crystal Growth & Design 8 (2008) 2497-2504.

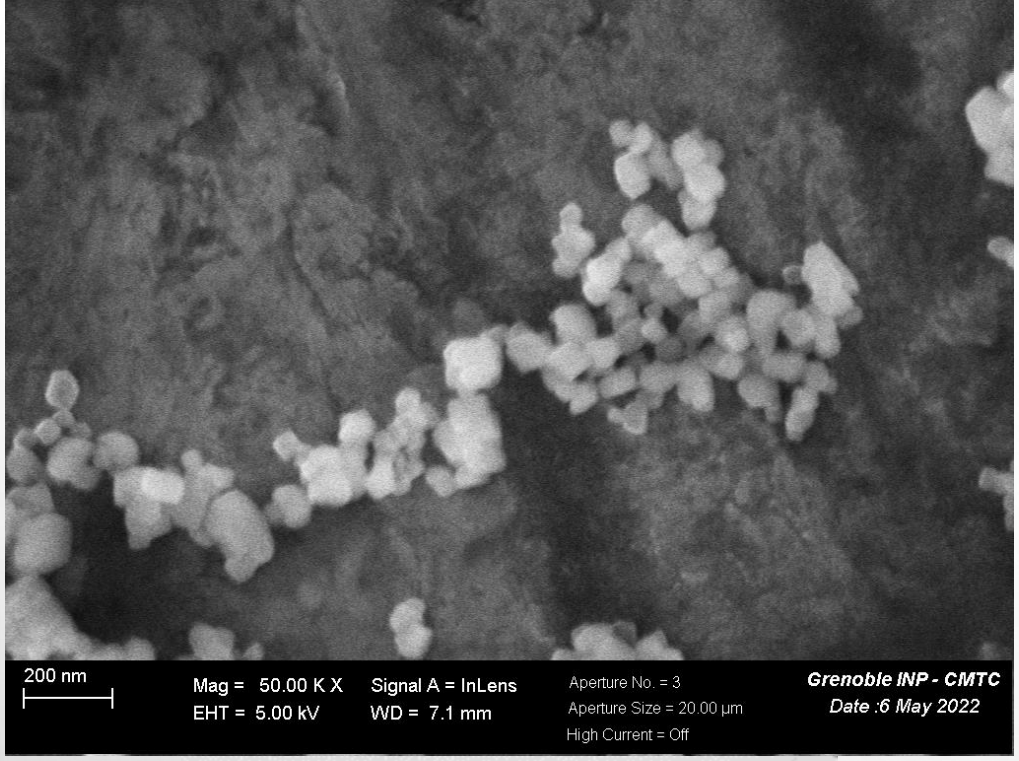

$CaCO_3$

ISTerre

Nano-calcite synthesis by aqueous and/or gas-solid carbonation

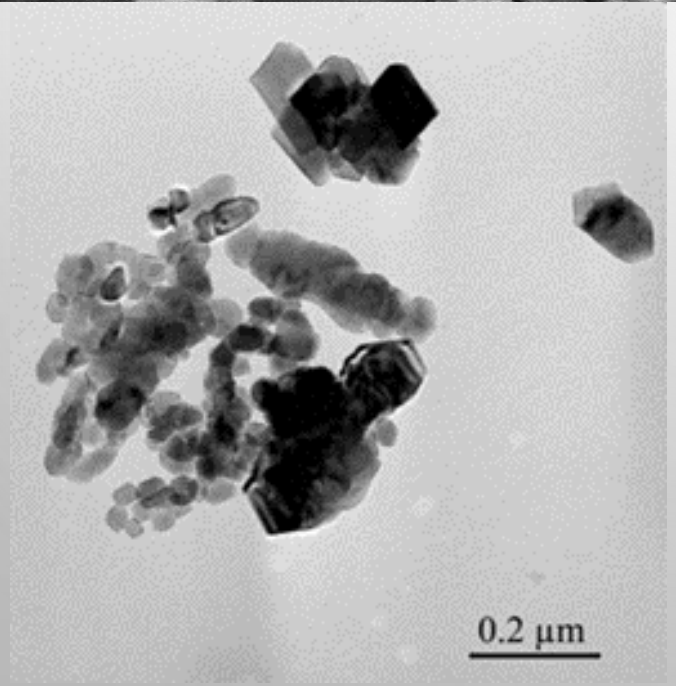

- G. Montes-Hernandez, F. Renard, N. Geffroy, L. Charlet, J. Pironon, Calcite precipitation from CO2-H2O-Ca(OH)2 slurry under high pressure of CO2. Journal of Crystal Growth 308 (2007) 228-236.

- G. Montes-Hernandez, D. Daval, R. Chiriac, F. Renard. Growth of nanosized calcite through gas-solid carbonation of nanosized portlandite particles under anisobaric conditions. Crystal Growth & Design 10 (2010) 4823-4830.

- G. Montes-Hernandez, A. Fernandez-Martinez, F. Renard, Novel Method to estimate the linear growth rate of submicrometric calcite produced in a triphasic gas-liquid-solid system. Crystal Growth & Design 9 (2009) 4567-4573.

Porous calcite mesocrystals by portlandite carbonation in presence of organic additives

$CaCO_3$

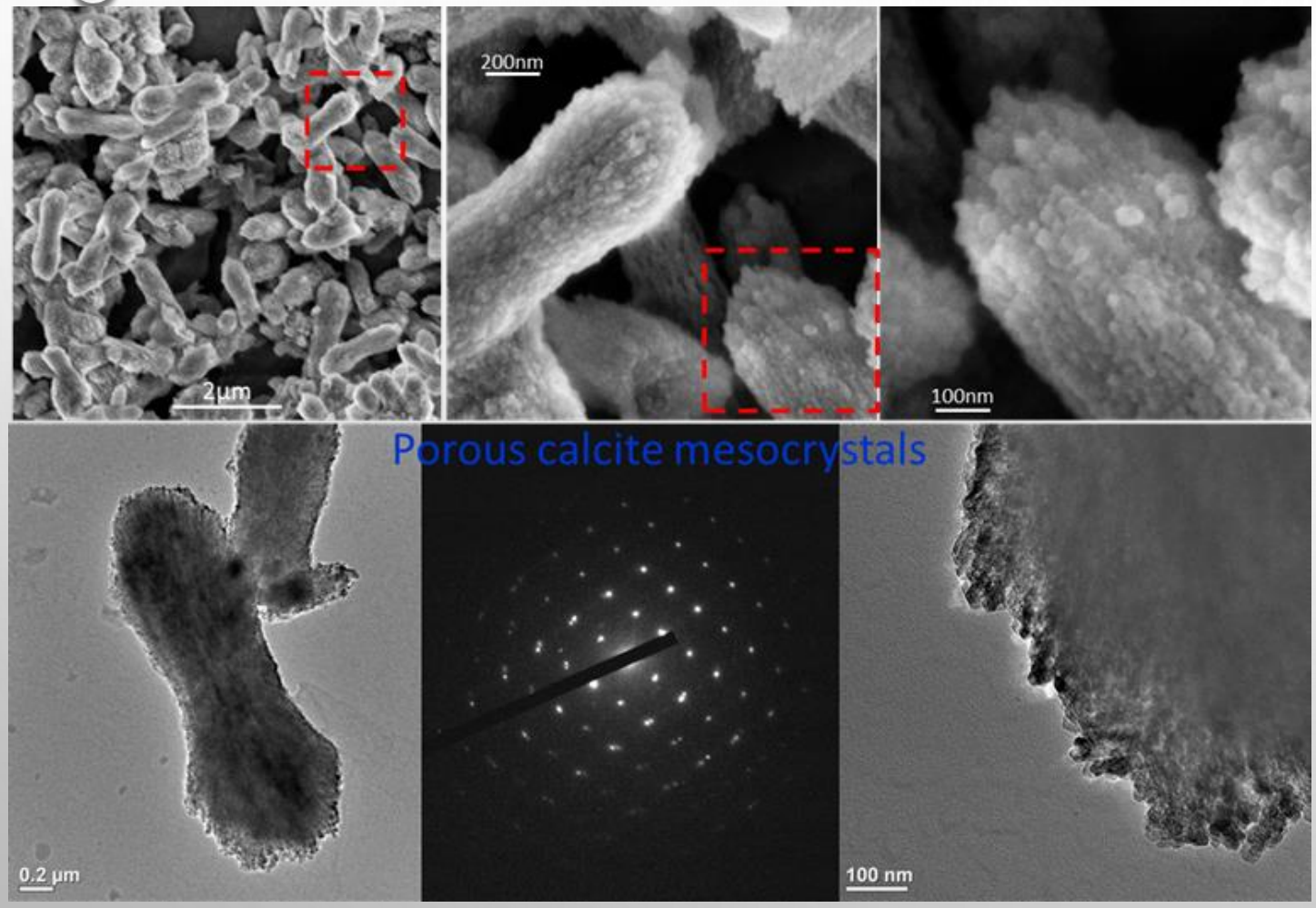

- G. Montes-Hernandez, F. Renard, N. Findling, A-L. Auzende. Formation of porous calcite mesocrystals from CO2-H2O-Ca(OH)2 slurry in the presence of common domestic drinks, CrystEngComm 17 (2015) 5725-5733.

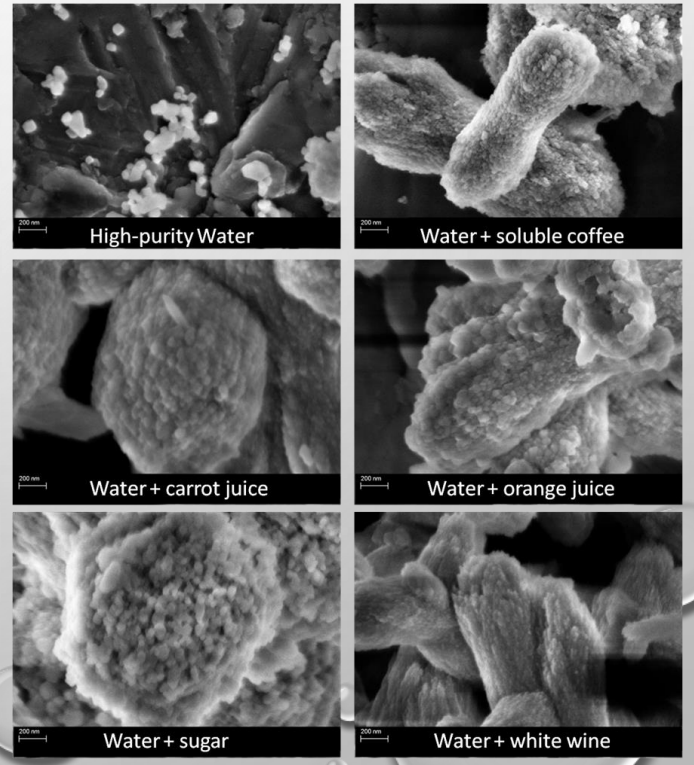

Acicular goethite synthesis with high specific surface area

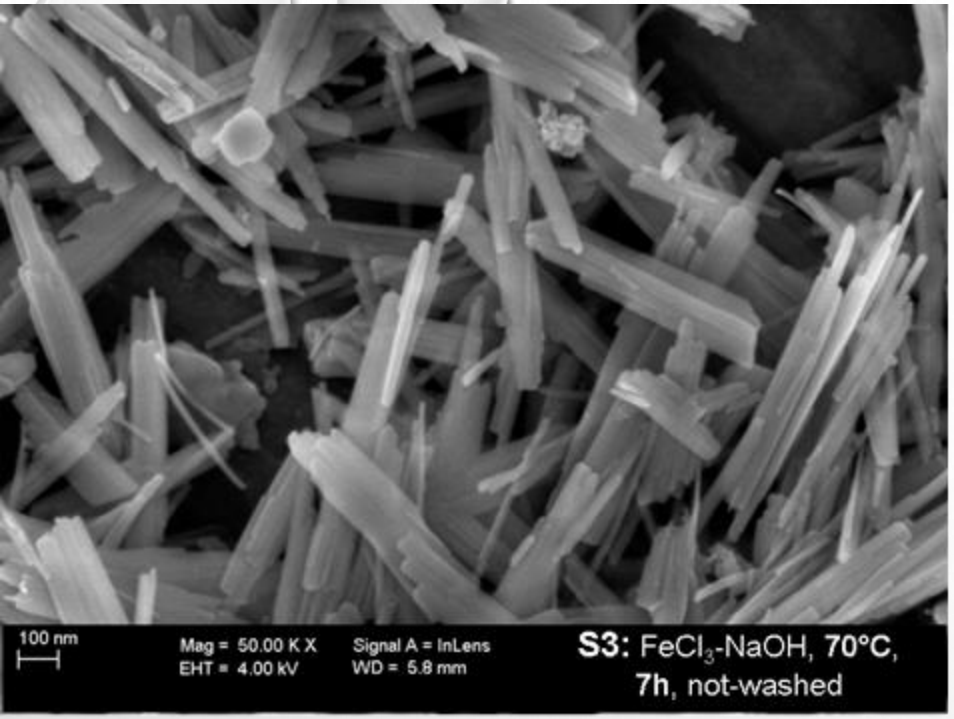

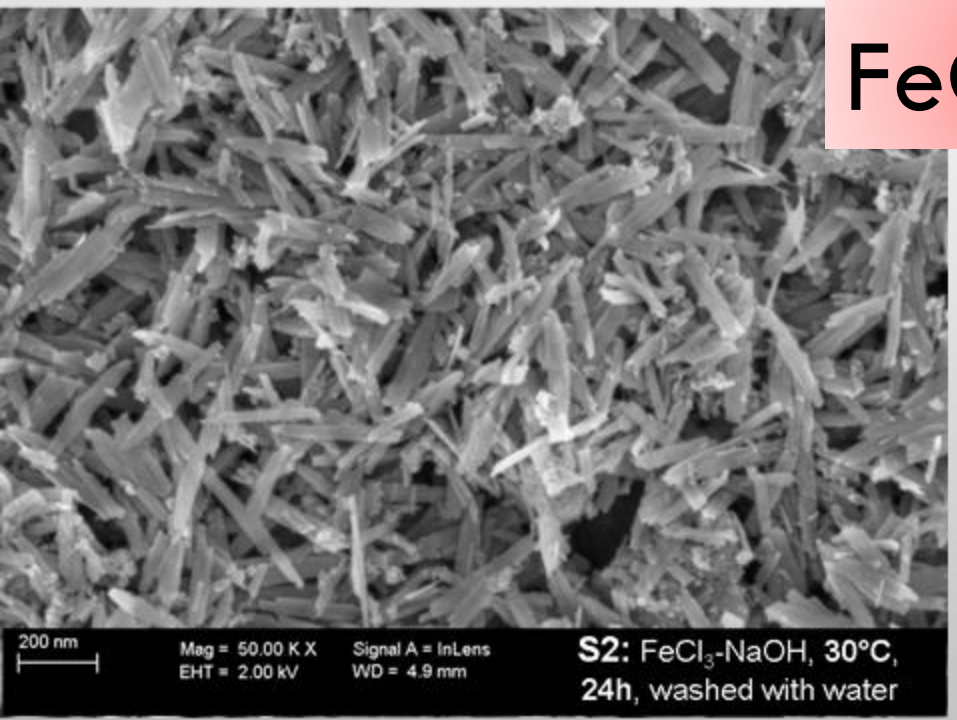

FeO(OH)

- G. Montes-Hernandez, P. Beck, F. Renard, E. Quirico, B. Lanson, R. Chiriac, N. Findling. Fast precipitation of acicular goethite from ferric hydroxide gel under moderate temperature (30 and 70 C degrees). Crystal Growth & Design 11 (2011) 2264-2272.

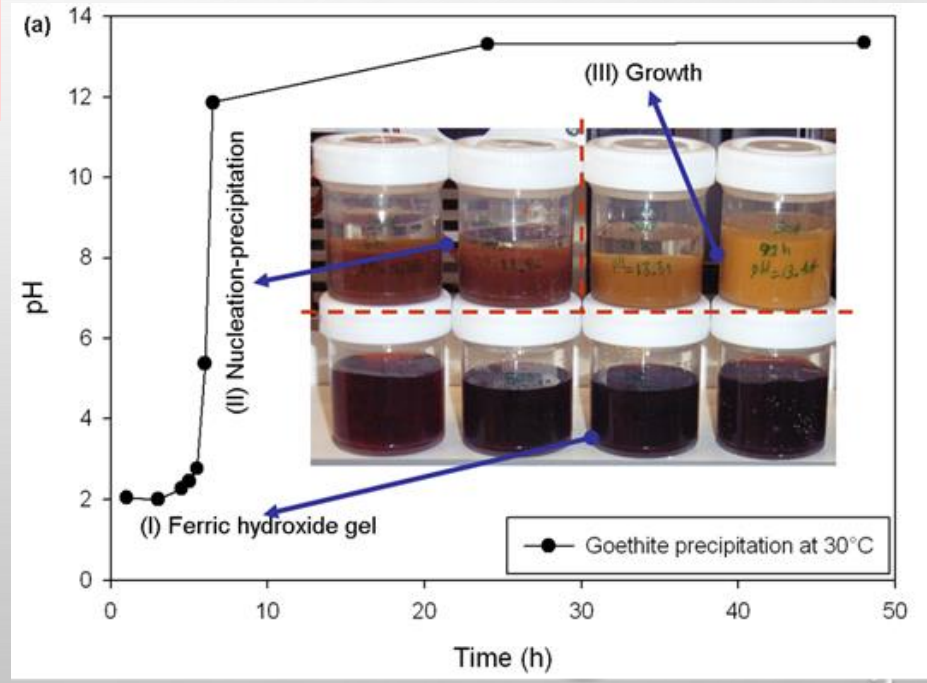

Synthesis of calcium iron oxide chloride hydrate (CaFe)

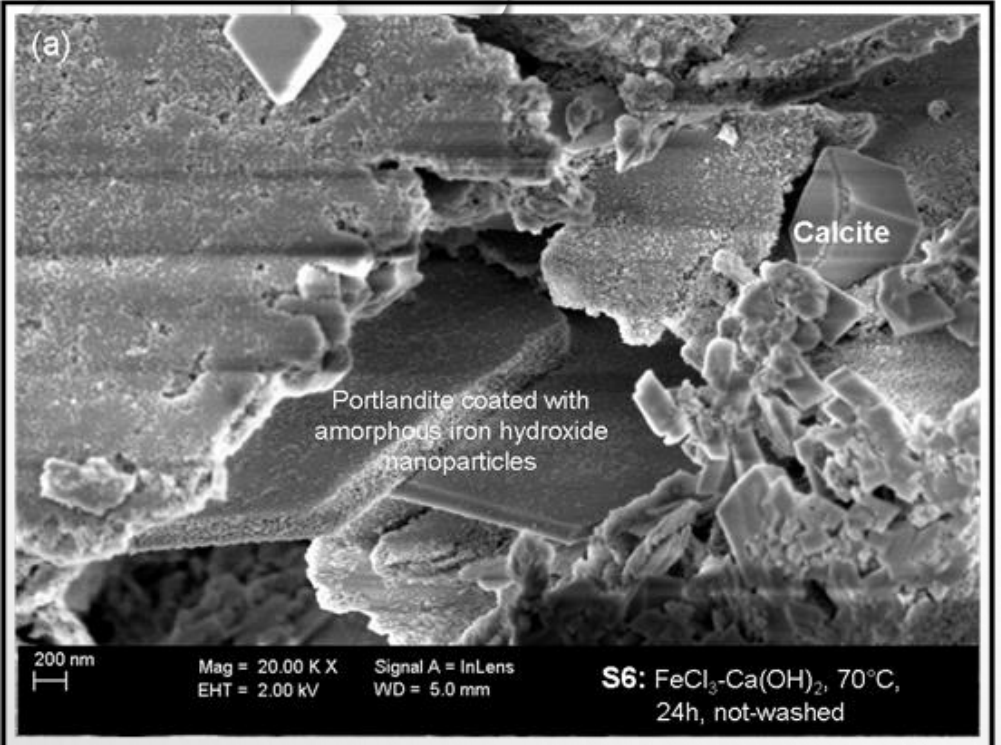

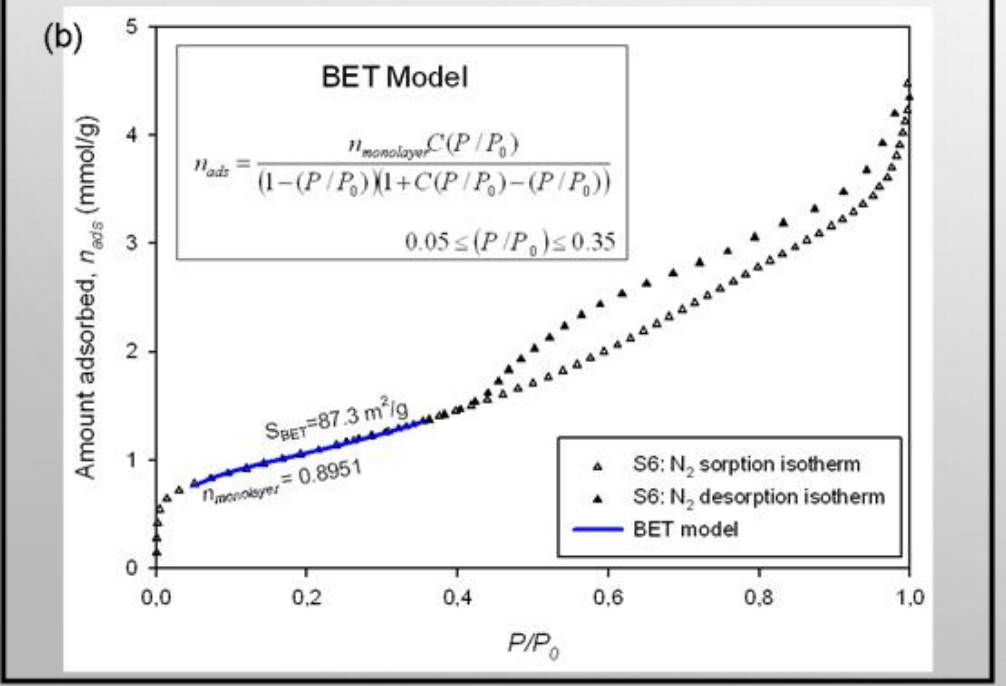

- G. Montes-Hernandez, P. Beck, F. Renard, E. Quirico, B. Lanson, R. Chiriac, N. Findling. Fast precipitation of acicular goethite from ferric hydroxide gel under moderate temperature (30 and 70 C degrees). Crystal Growth & Design 11 (2011) 2264-2272.

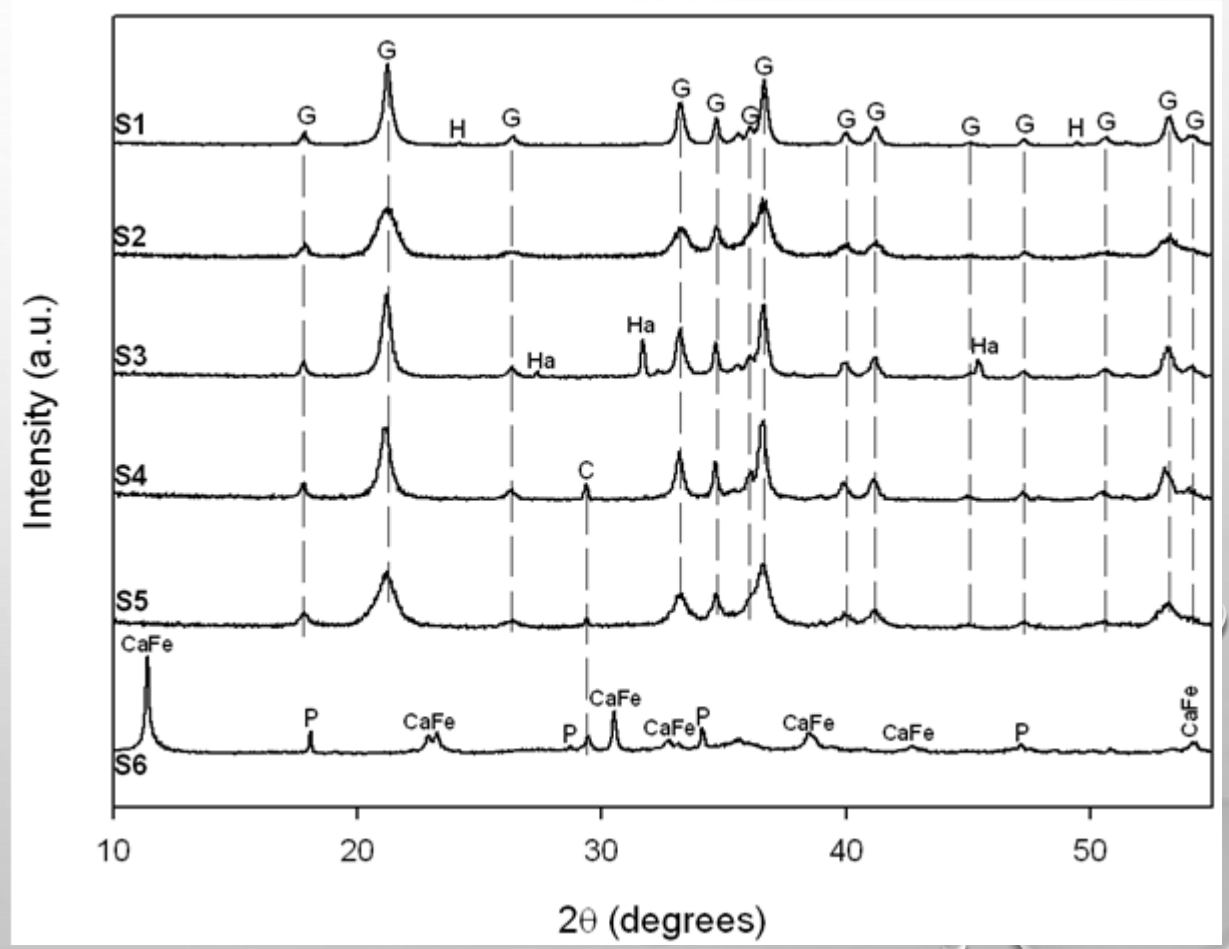

Synthesis of goethite-calcite composite with high S_{BET}

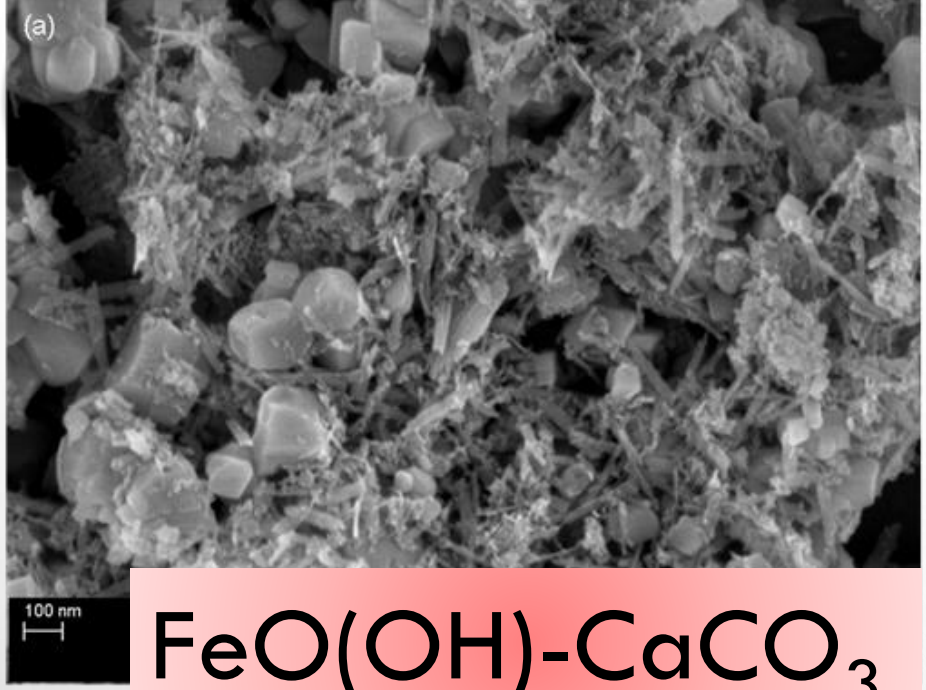

$FeO(OH)$-$CaCO_3$

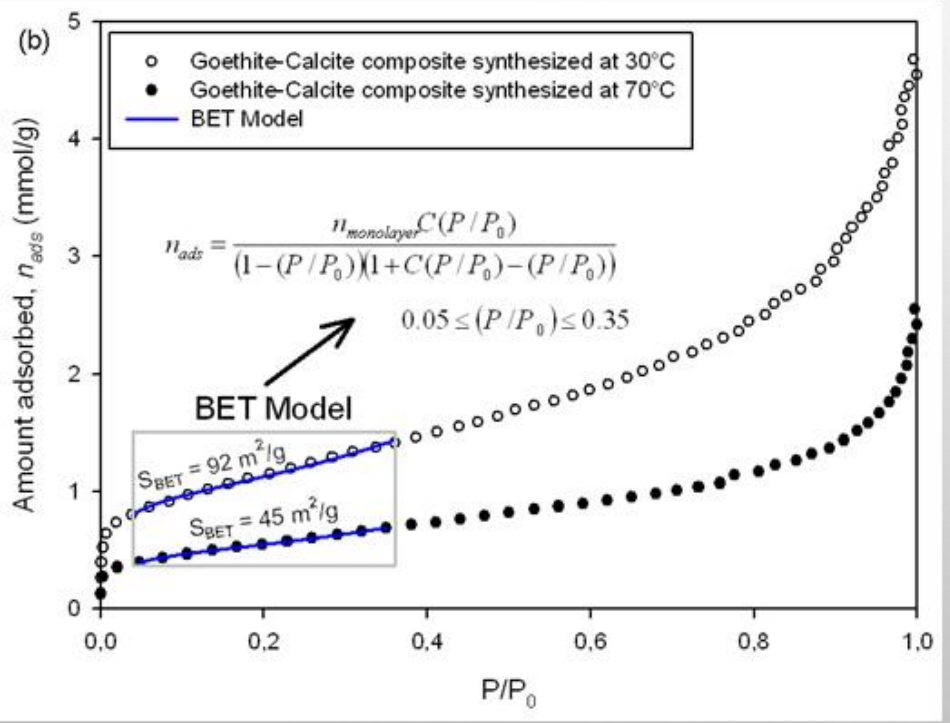

- G. Montes-Hernandez, F. Renard, R. Chiriac, N. Findling, J. Ghanbaja, F. Toche. Sequential precipitation of a new goethite-calcite nanocomposite and its possible application in the removal of toxic ions from polluted water. Chemical Engineering Journal 214 (2013) 139-148

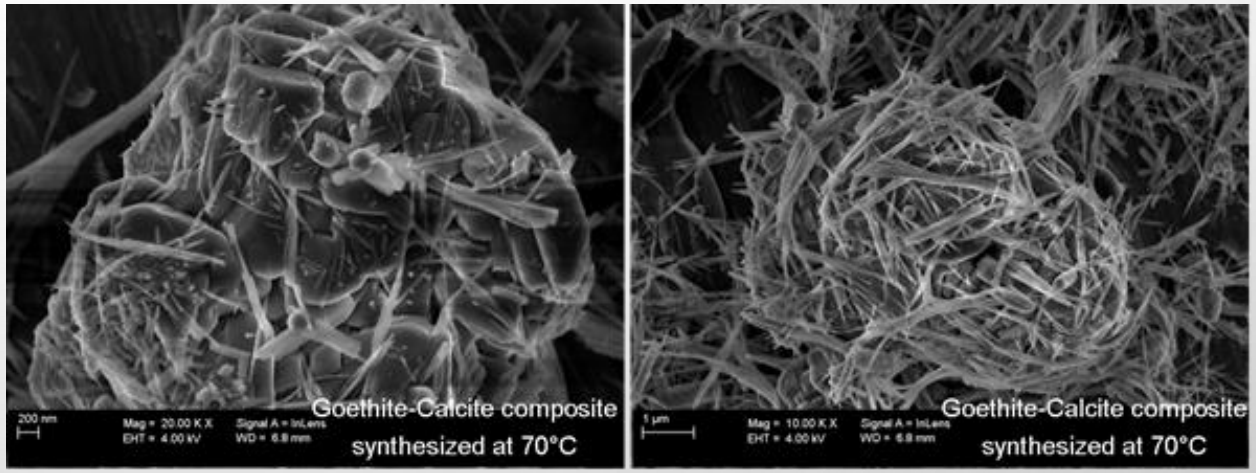

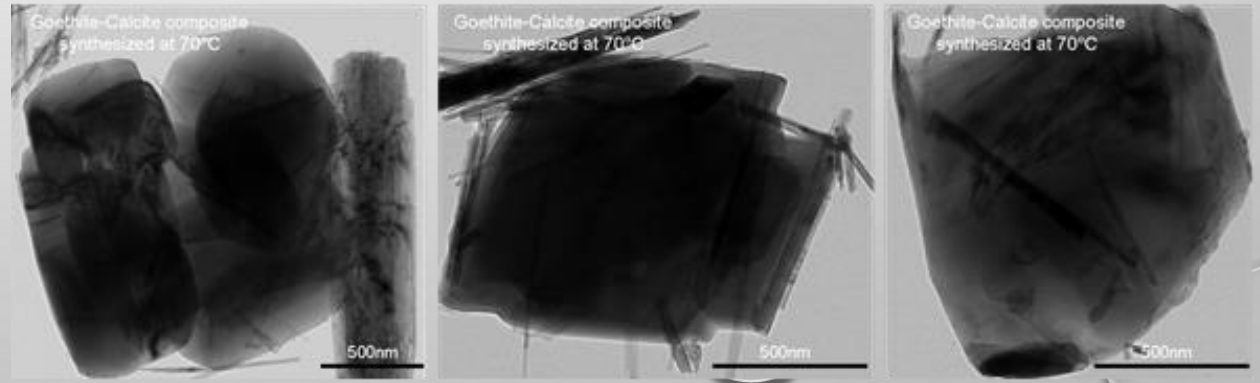

Synthesis of hydromagnesite and magnesite under mild conditions (T≤90°C)

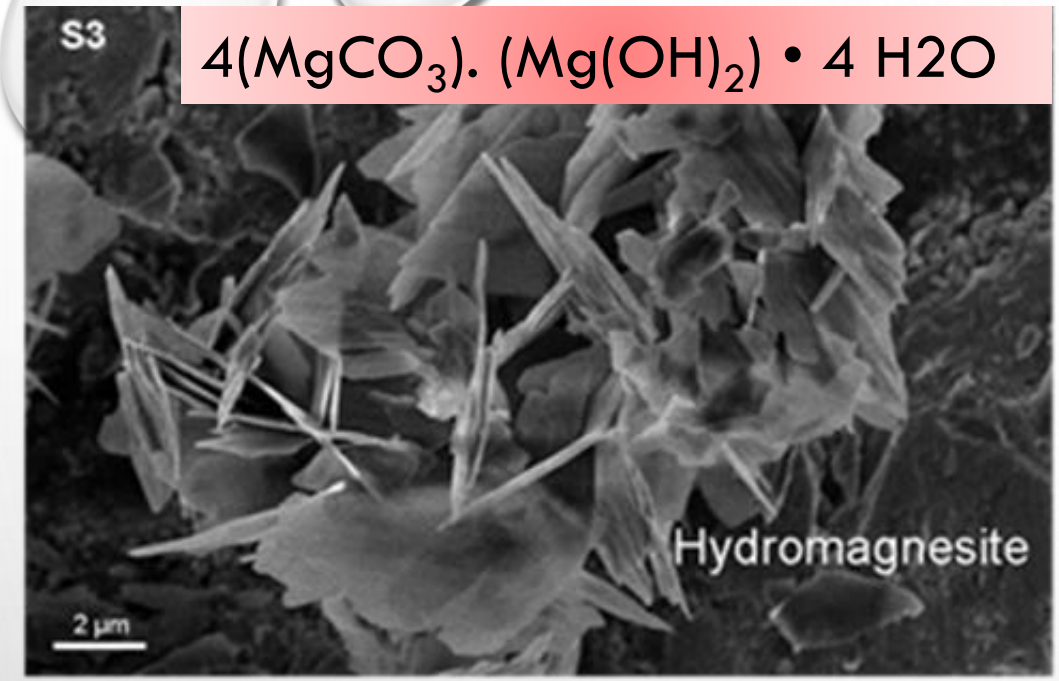

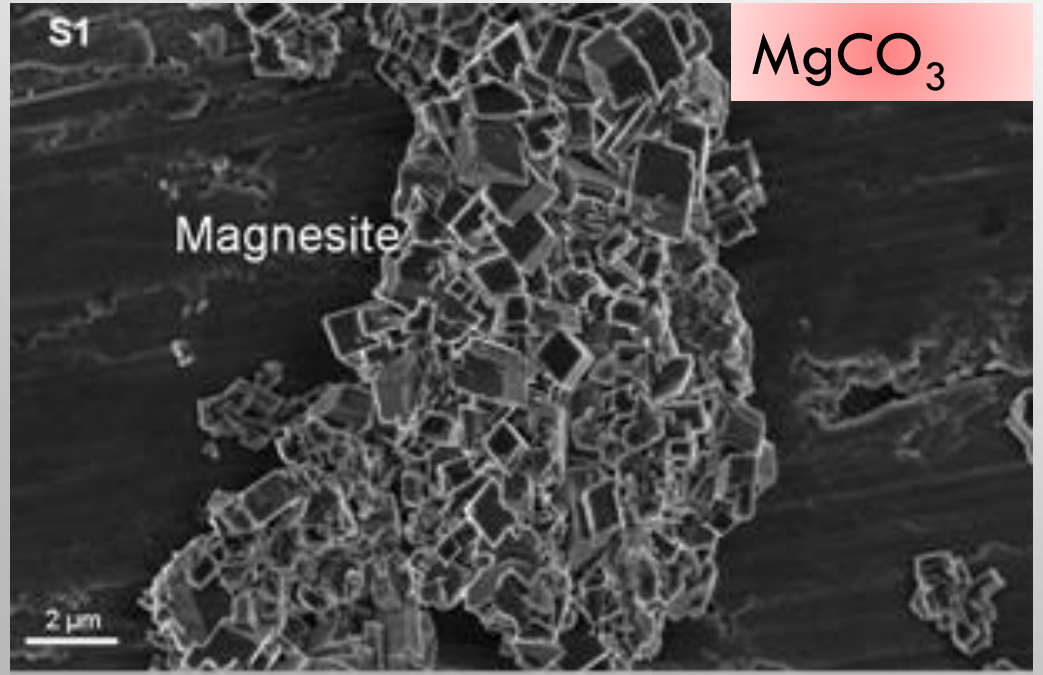

- German Montes-Hernandez. Magnesite Formation from Nesquehonite Slurry at 90°C using some Soluble Mg Salts : Eitelite as an Atypical Transient Mineral Phase Chemical Engineering Science 287 (2024) 119776
- G. Montes-Hernandez, M. Bah, F. Renard. Mechanism of the formation of engineered magnesite : A useful mineral to mitigate CO2 industrial emissions. Journal of CO2 utilization 35 (2020) 272-276.
- G. Montes-Hernandez, F. Renard. Time-resolved in situ Raman spectroscopy of the nucleation and growth of siderite, magnesite and calcite and their precursors. Crystal Growth & Design 16 (2016) 7218-7230.
- G. Montes-Hernandez, F. Renard, R. Chiriac, N. Findling, F. Toche. Rapid precipitation of magnesite micro-crystals from Mg(OH)2-H2O-CO2 slurry enhanced by NaOH and a heat-ageing step (from 20 to 90°C). Crystal Growth & Design 12 (2012) 5233-5240.

Synthesis of Eitelite under mild conditions (T≤90°C)

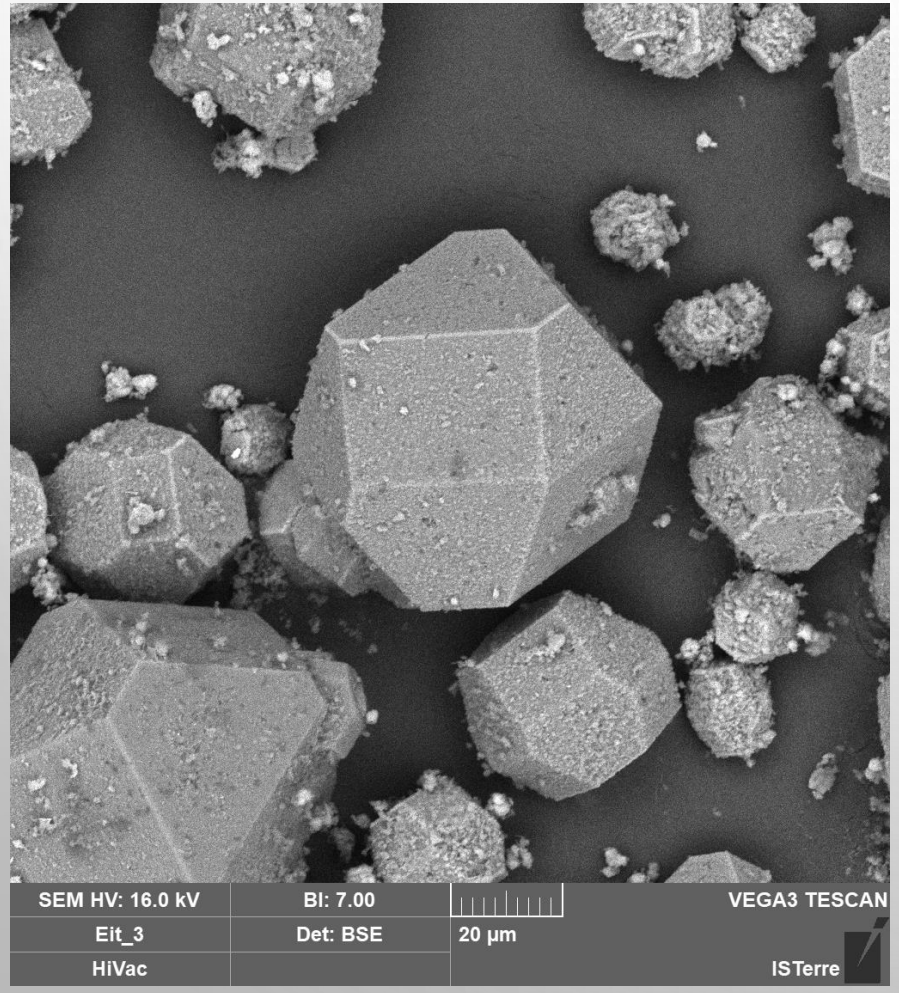

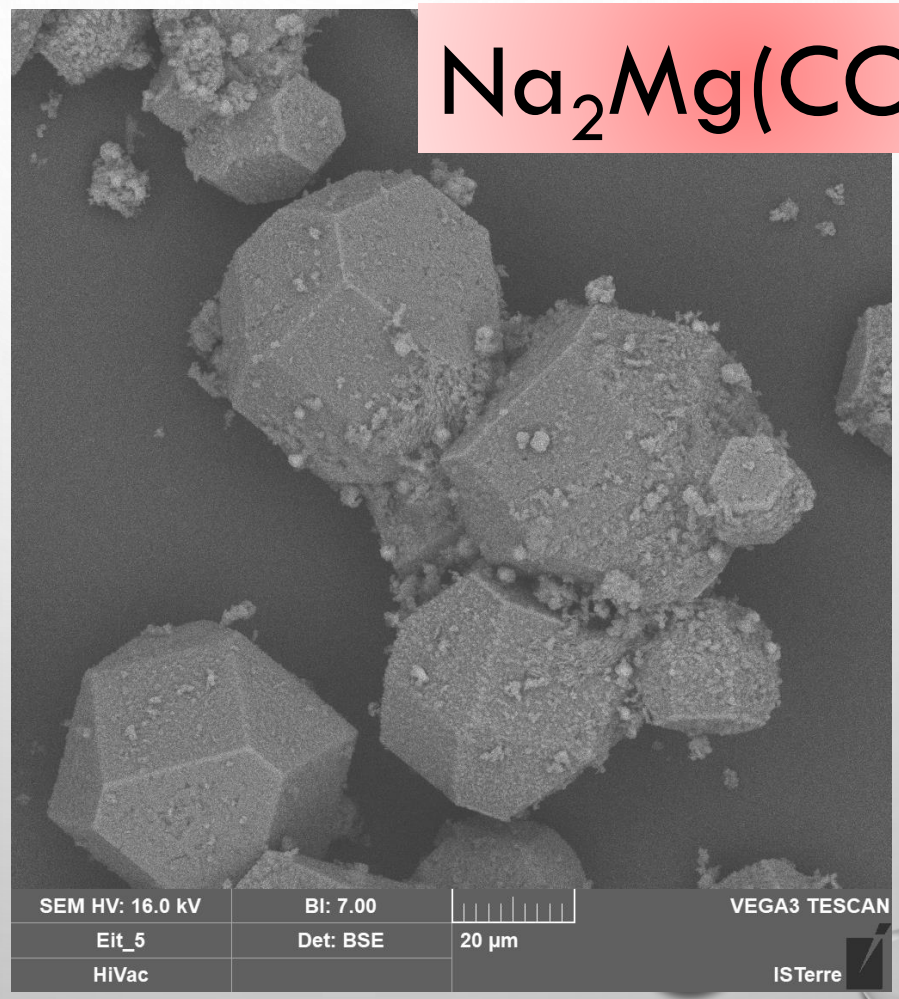

$Na_2Mg(CO_3)_2$

- German Montes-Hernandez. Magnesite Formation from Nesquehonite Slurry at 90°C using some Soluble Mg Salts : Eitelite as an Atypical Transient Mineral Phase Chemical Engineering Science 287 (2024) 119776

Synthesis of Nesquehonite and Dypingite at room T

$MgCO_3.3H_2O$

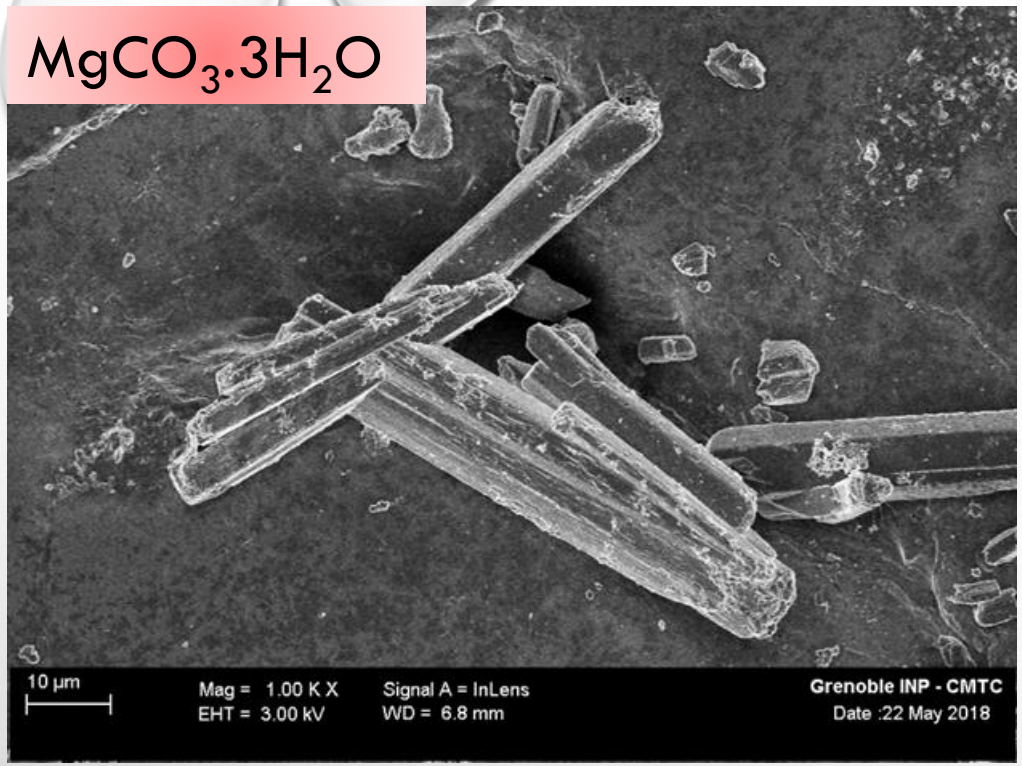

- G. Montes-Hernandez, F. Renard. Time-resolved in situ Raman spectroscopy of the nucleation and growth of siderite, magnesite and calcite and their precursors. Crystal Growth & Design 16 (2016) 7218-7230.
- G. Montes-Hernandez, F. Renard, R. Chiriac, N. Findling, F. Toche. Rapid precipitation of magnesite micro-crystals from Mg(OH)2-H2O-CO2 slurry enhanced by NaOH and a heat-ageing step (from 20 to 90°C). Crystal Growth & Design 12 (2012) 5233-5240.

$4(MgCO_3).(Mg(OH)_2) \cdot 5\ H2O$

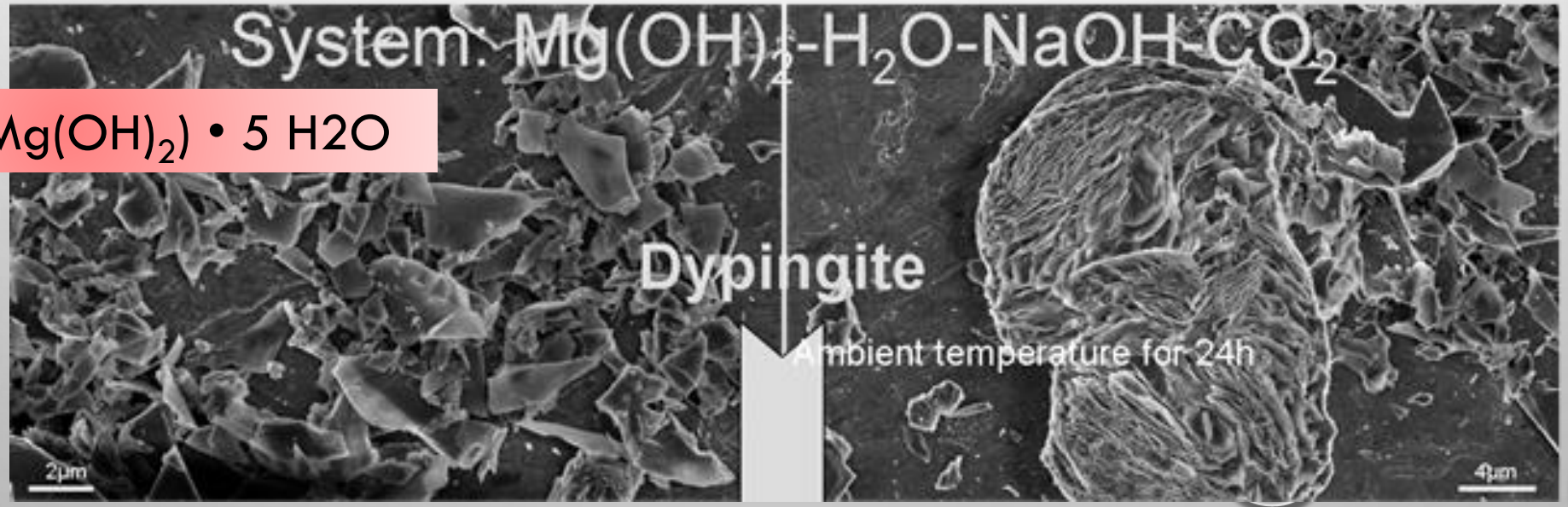

Synthesis of Siderite by precipitation at room T

$FeCO_3$

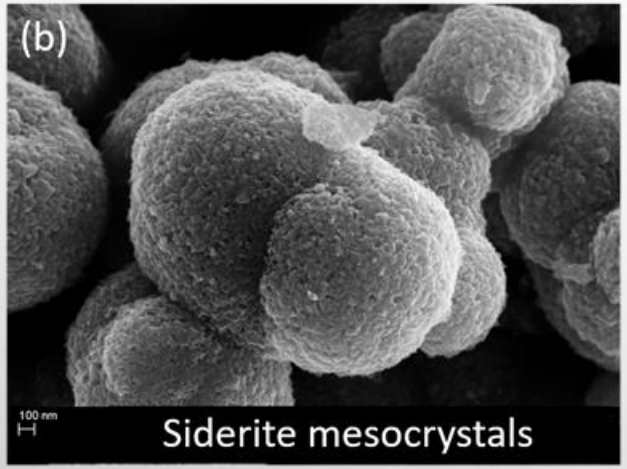

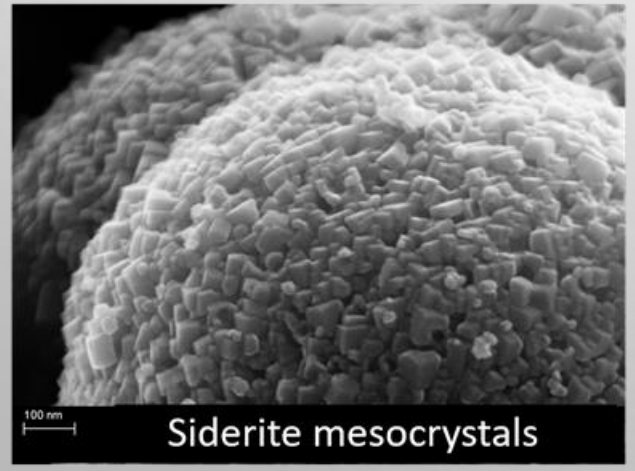

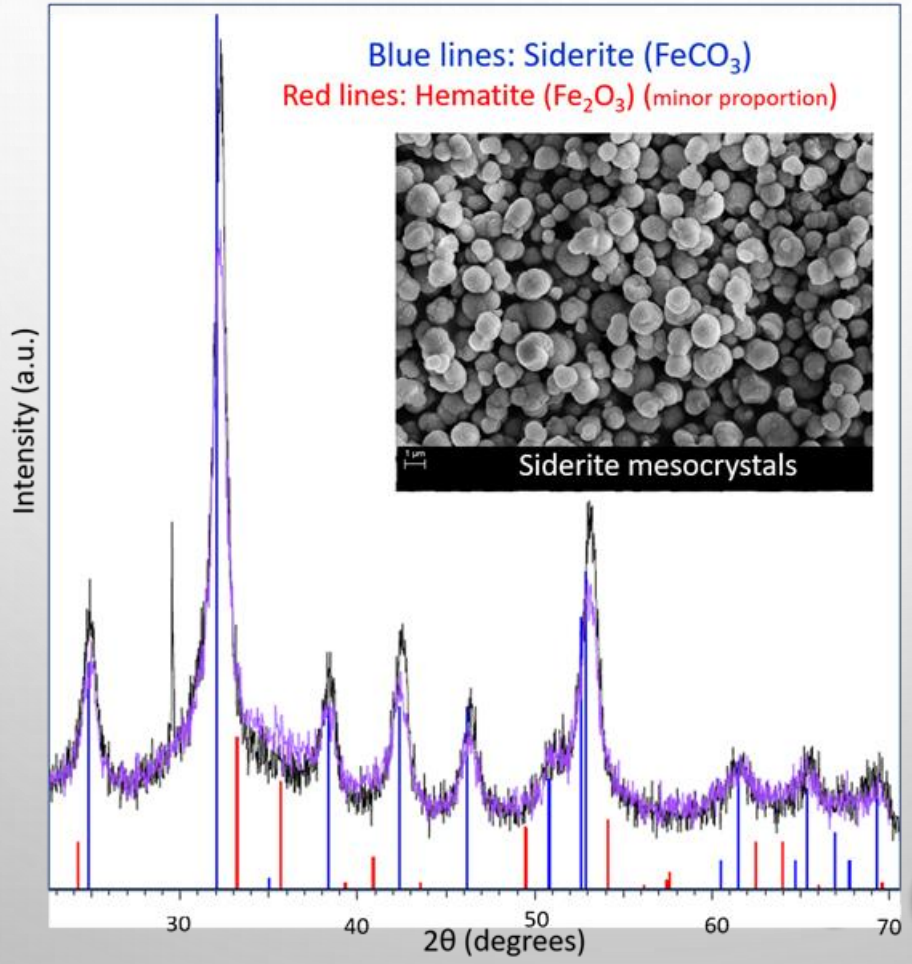

- G. Montes-Hernandez, F. Renard. Time-resolved in situ Raman spectroscopy of the nucleation and growth of siderite, magnesite and calcite and their precursors. Crystal Growth & Design 16 (2016) 7218-7230.

- S. Hajji, G. Montes-Hernandez, G. Sarret, A. Tordo, G. Morin, G. Ona-Nguema, S. Bureau, T. Turki, M. Nzoughi. Arsenite and chromate sequestration onto ferrihydrite, siderite and goethite nanostructured minerals : Isotherms from flow-through reactor experiments and XAS measurements. Journal of Hazardous Materials 362 (2019) 358-367

Synthesis of ferrihydrite 6L by oxidative decomposition of siderite at 60°C in oven

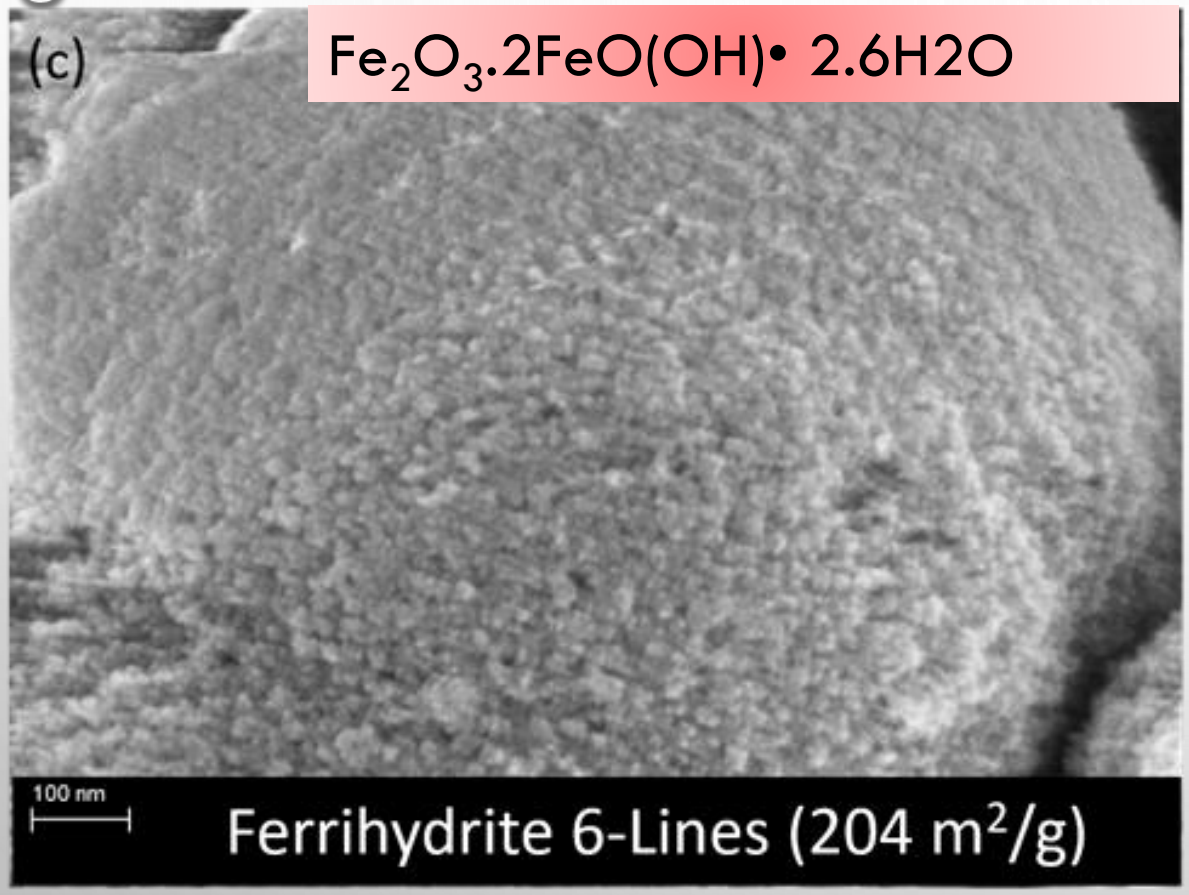

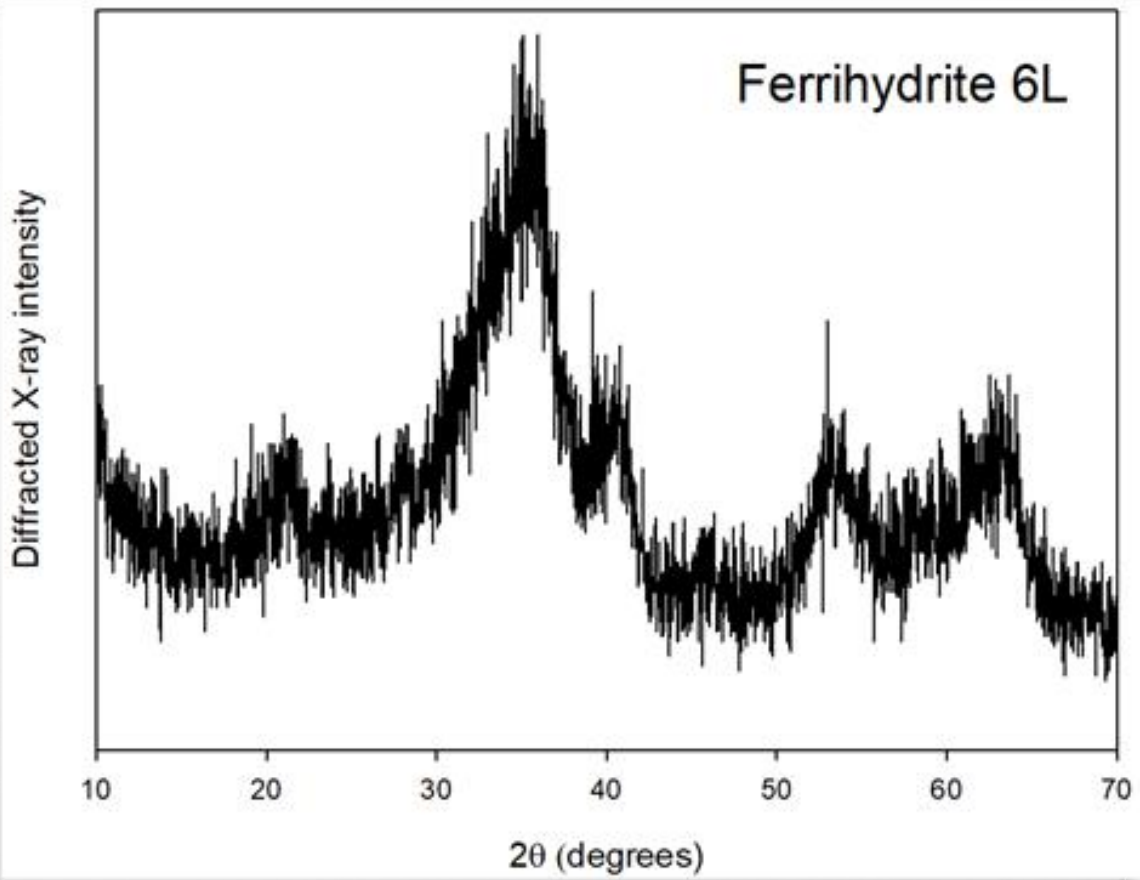

- S. Hajji, G. Montes-Hernandez, G. Sarret, A. Tordo, G. Morin, G. Ona-Nguema, S. Bureau, T. Turki, M. Nzoughi. Arsenite and chromate sequestration onto ferrihydrite, siderite and goethite nanostructured minerals : Isotherms from flow-through reactor experiments and XAS measurements. Journal of Hazardous Materials 362 (2019) 358-367

Synthesis of Brushite and hydroxyapatite at room T

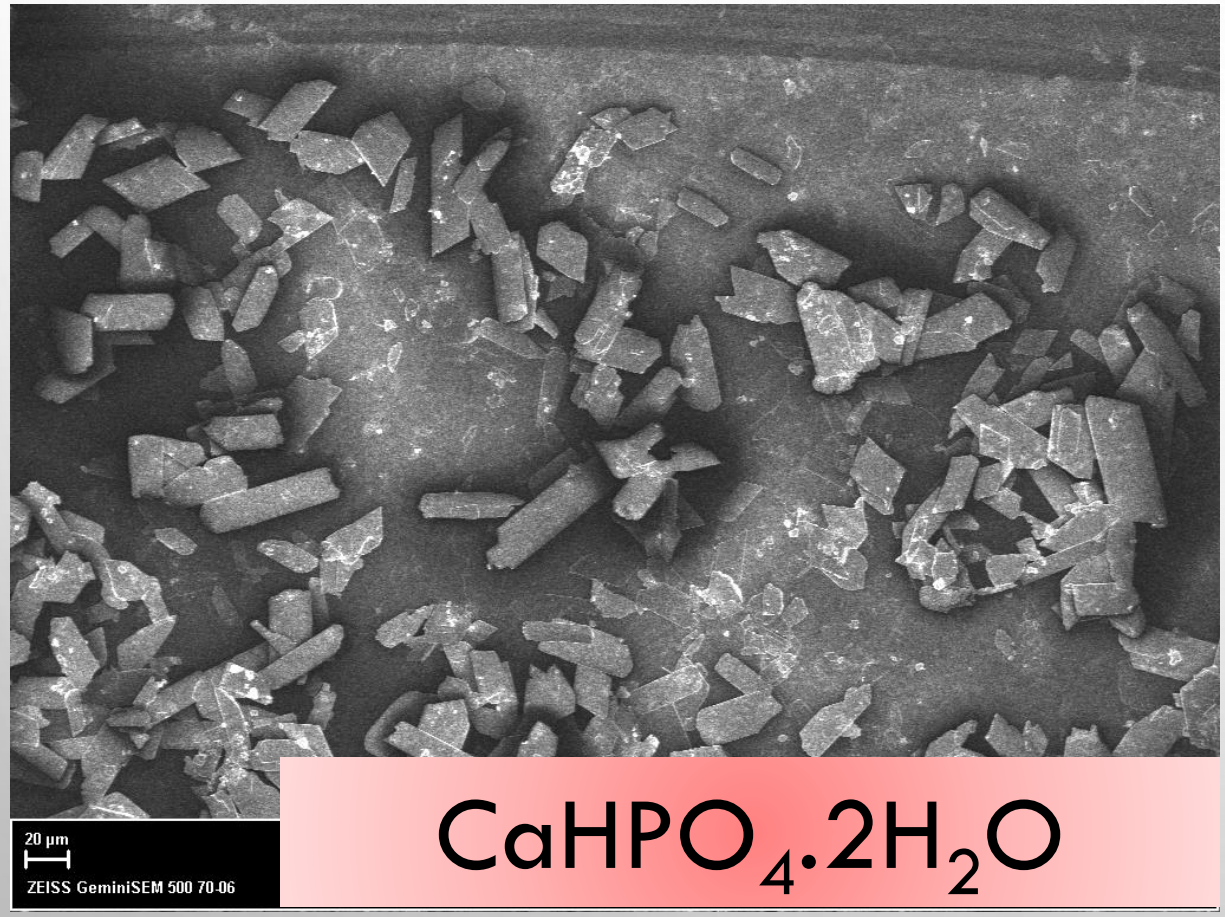

$CaHPO_4.2H_2O$

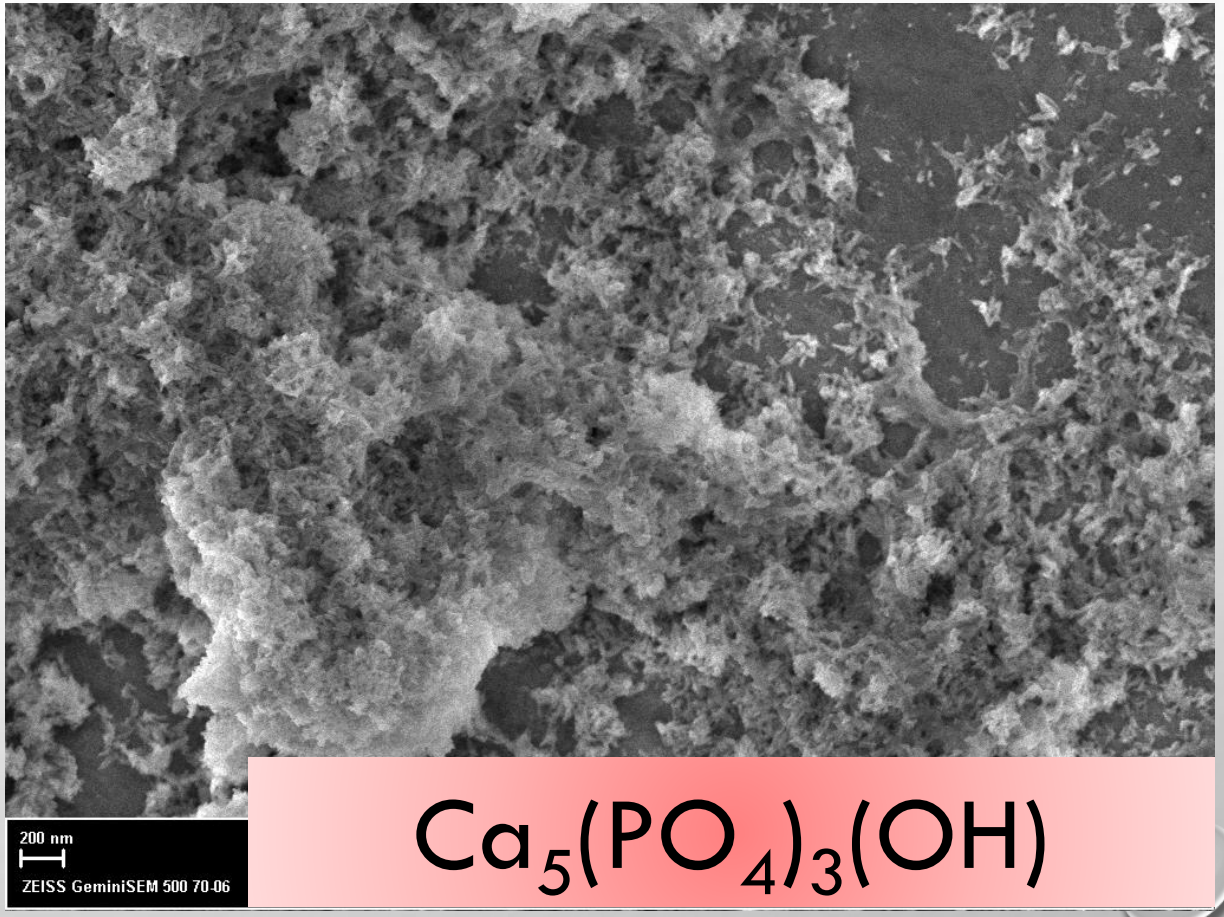

$Ca_5(PO_4)_3(OH)$

- G. Montes-Hernandez, F. Renard. Nucleation of Brushite and Hydroxyapatite from Amorphous Calcium Phosphate Phases Revealed by Dynamic in situ Raman Spectroscopy. The Journal of Physical Chemistry C 124 (2020) 15302-15311.

Synthesis of proto-dolomite and dolomite at room T or under hydrothermal conditions

$2Ca_{0.5}Mg_{0.5}CO_3.nH_2O \rightarrow CaMg(CO_3)_2 + 2nH_2O$

$CaMg(CO_3)_2$

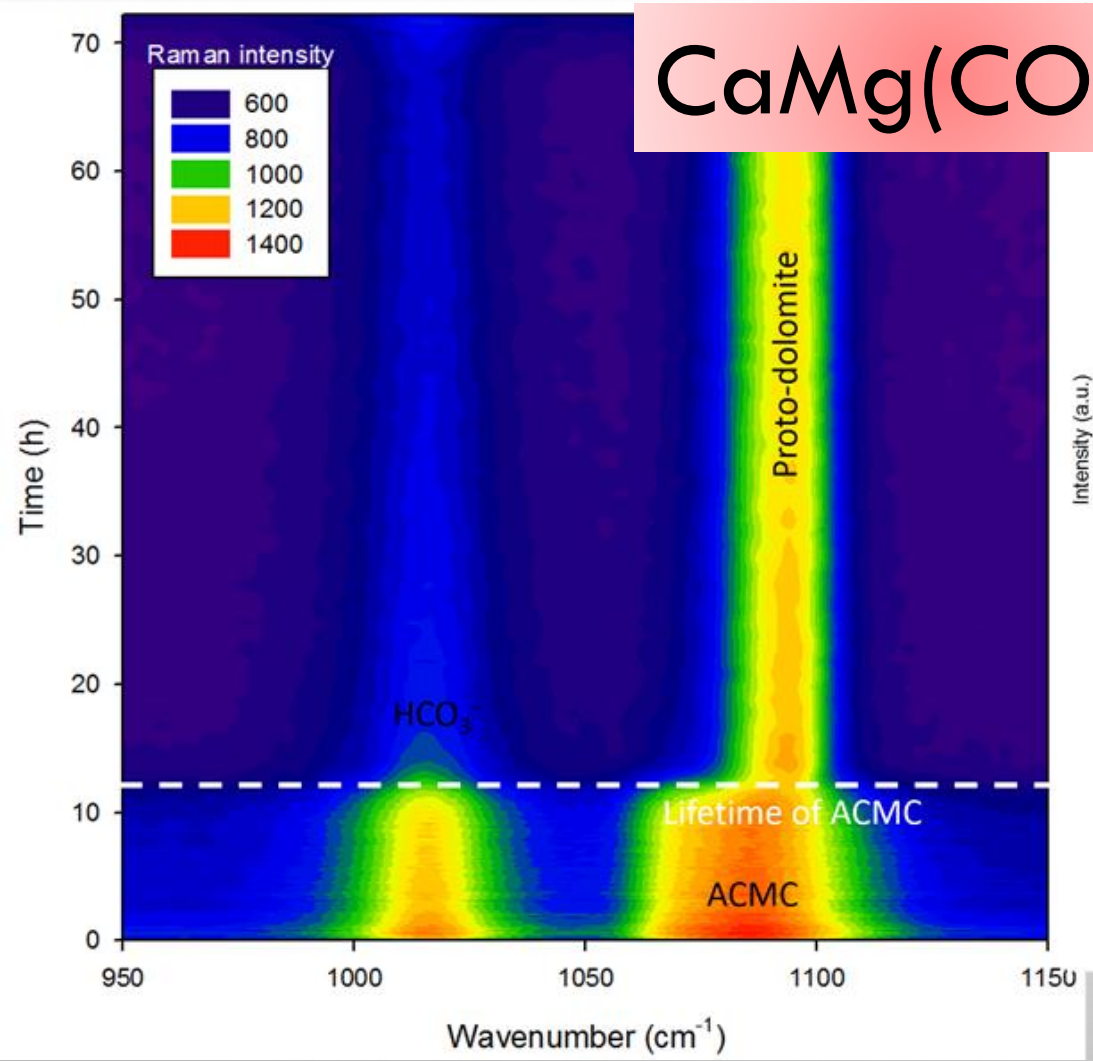

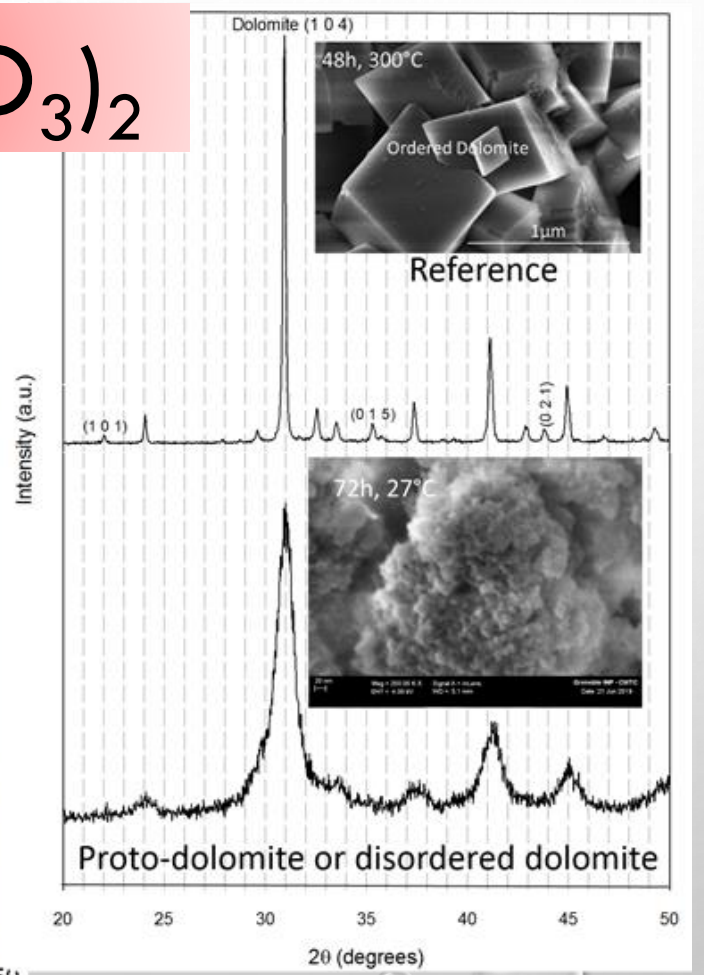

- G. Montes-Hernandez, F. Renard, A.L. Auzende, N. Findling. Amorphous calcium-magnesium carbonate (ACMC) accelerates dolomitization at room temperature under abiotic conditions. Crystal Growth & Design 20 (2020) 1434-1441.

- G. Montes-Hernandez, N. Findling, Renard. Dissolution-precipitation reactions controlling fast formation of dolomite under hydrothermal conditions. Applied Geochemistry 73 (2016) 169-177.

Synthesis of low and/or high Mg-Calcite and high Ca-magnesite

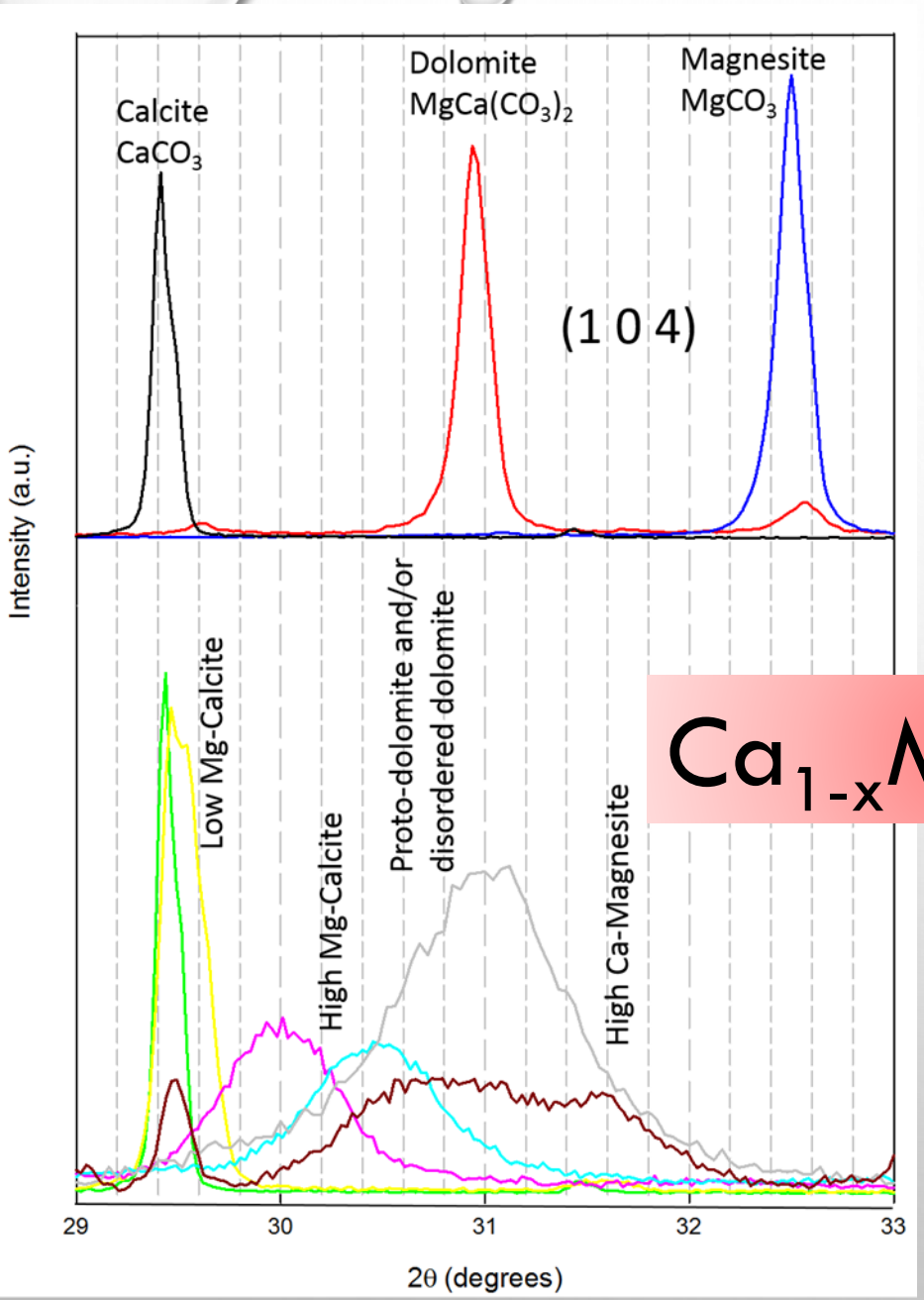

$Ca_{1-x}Mg_xCO_3$

- G. Montes-Hernandez, F. Renard, A.L. Auzende, N. Findling. Amorphous calcium-magnesium carbonate (ACMC) accelerates dolomitization at room temperature under abiotic conditions. Crystal Growth & Design 20 (2020) 1434-1441.

- G. Montes-Hernandez, N. Findling, Renard. Dissolution-precipitation reactions controlling fast formation of dolomite under hydrothermal conditions. Applied Geochemistry 73 (2016) 169-177.

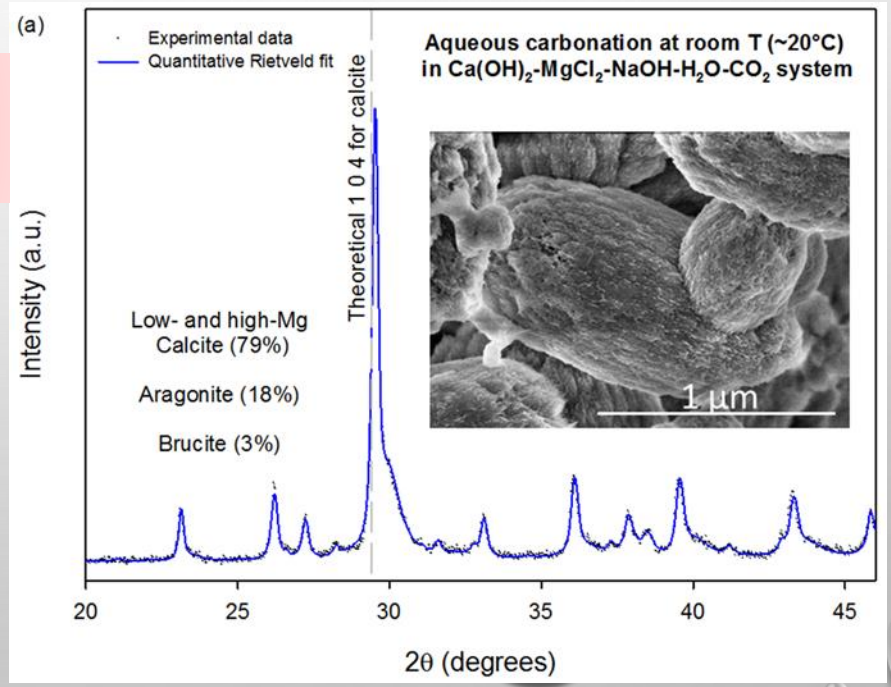

Synthesis of bastnäsite under mild and hydrothermal conditions

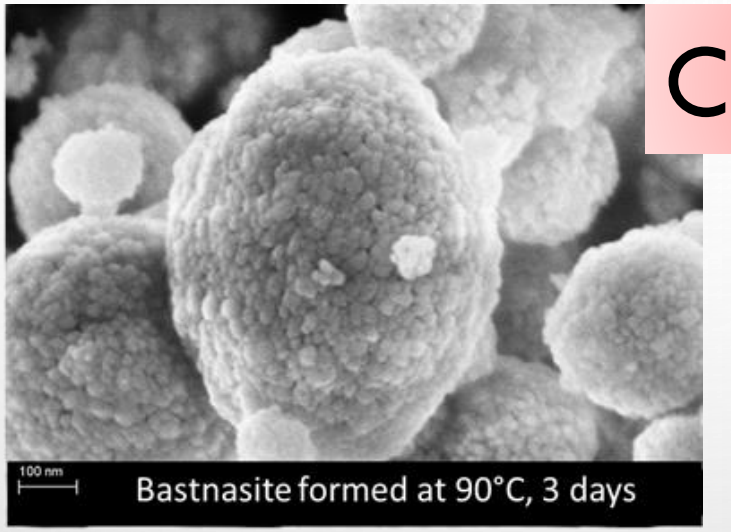

$CeCO_3F$

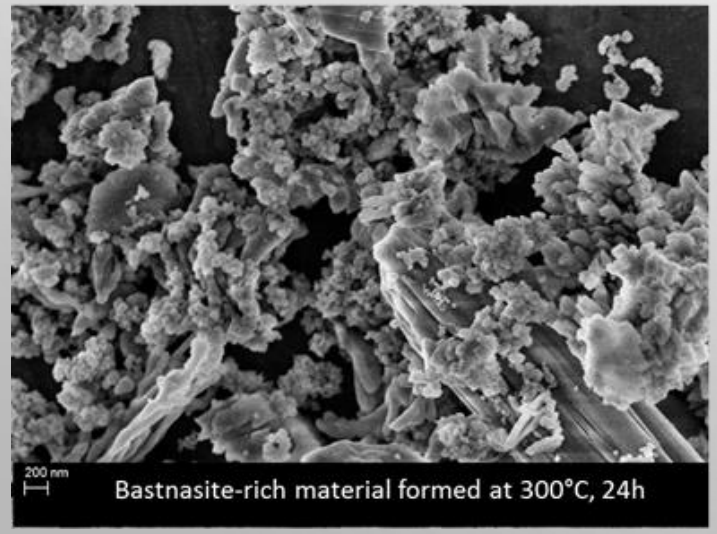

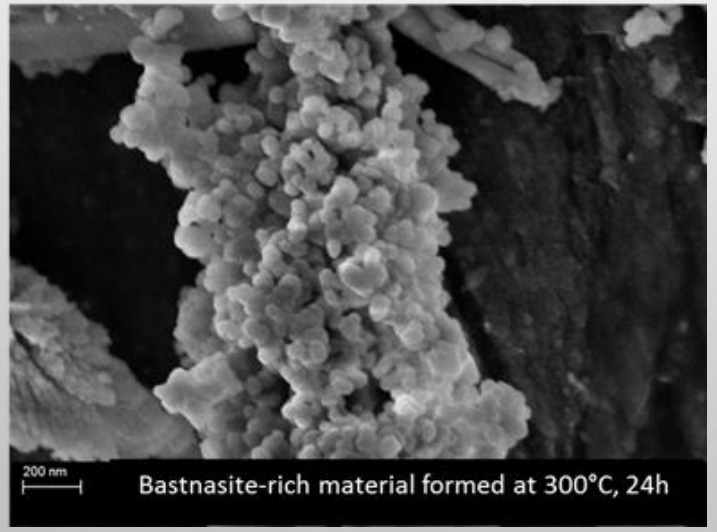

- G. Montes-Hernandez, R. Chiriac, N. Findling, F. Toche, F. Renard. Synthesis of Ceria (CeO2 and CeO2-x) Nanoparticles via Decarbonation and Ce(III) Oxydation of Synthetic Bastnäsite (CeCO3F). Materials Chemistry and Physics 172 (2016) 202-210.

- G. Montes-Hernandez. Synthesis of Magnetite, Ceria and Magnetite-Ceria Materials by Calcination of Nanostructured Precursor-Minerals. Materials Letters 276 (2020) 128246.

Synthesis of ceria by calcination of bastnäsite with and without secondary vacuum

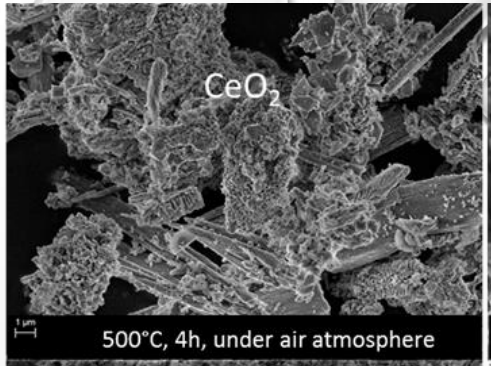

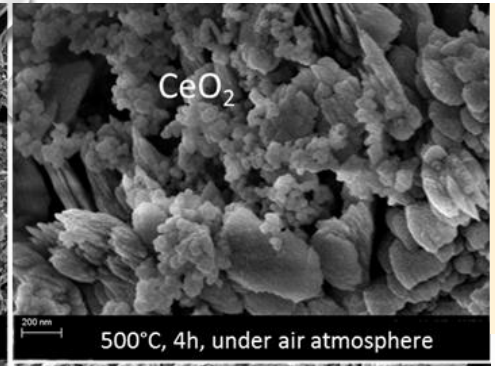

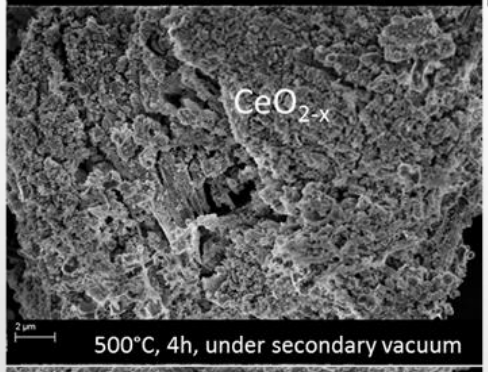

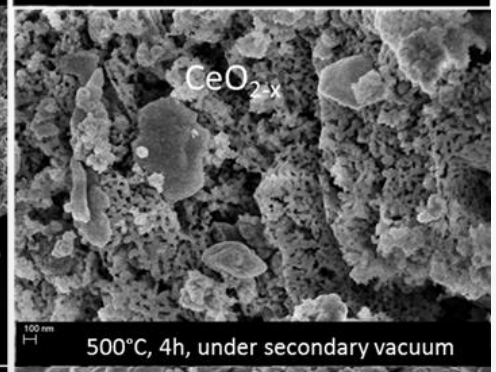

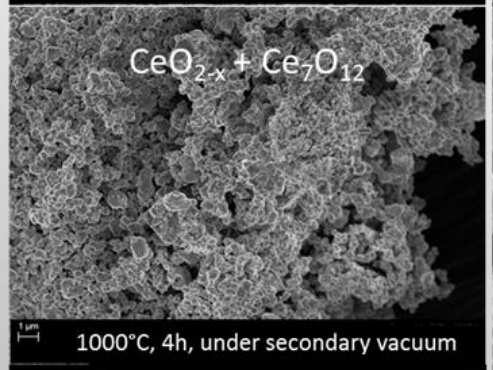

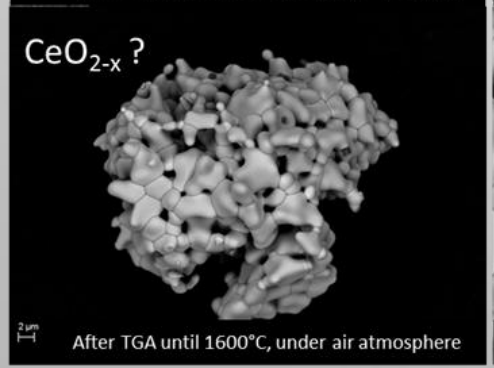

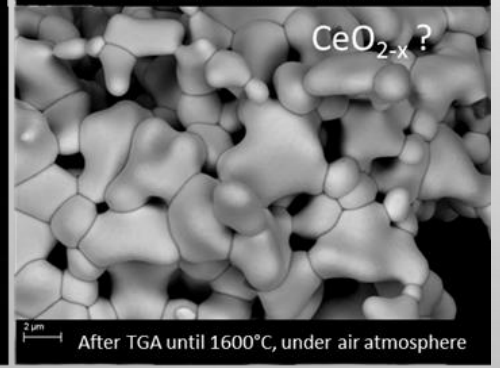

- G. Montes-Hernandez, R. Chiriac, N. Findling, F. Toche, F. Renard. Synthesis of Ceria (CeO2 and CeO2-x) Nanoparticles via Decarbonation and Ce(III) Oxydation of Synthetic Bastnäsite (CeCO3F). Materials Chemistry and Physics 172 (2016) 202-210.

- G. Montes-Hernandez. Synthesis of Magnetite, Ceria and Magnetite-Ceria Materials by Calcination of Nanostructured Precursor-Minerals. Materials Letters 276 (2020) 128246.

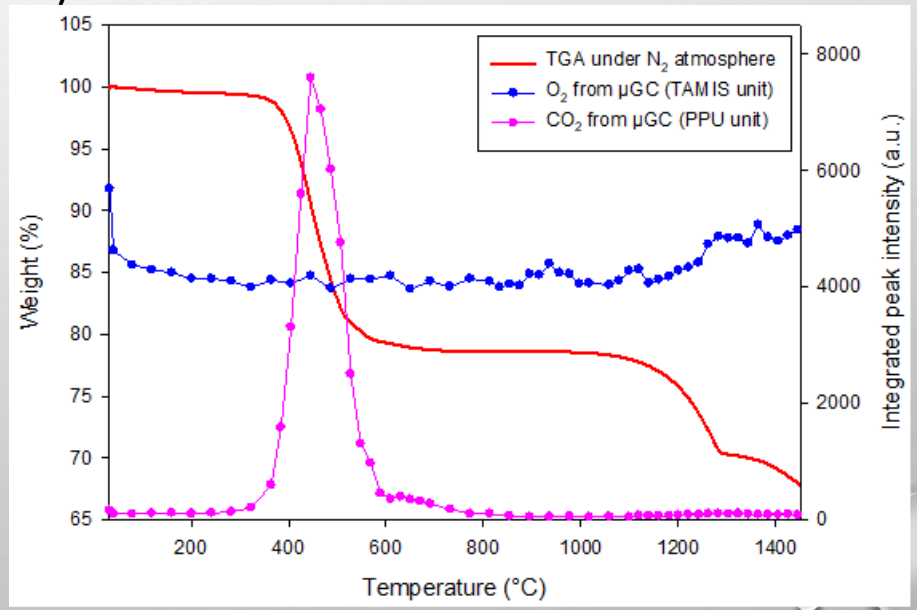

Synthesis of magnetite by partial Fe(III) reduction during calcination

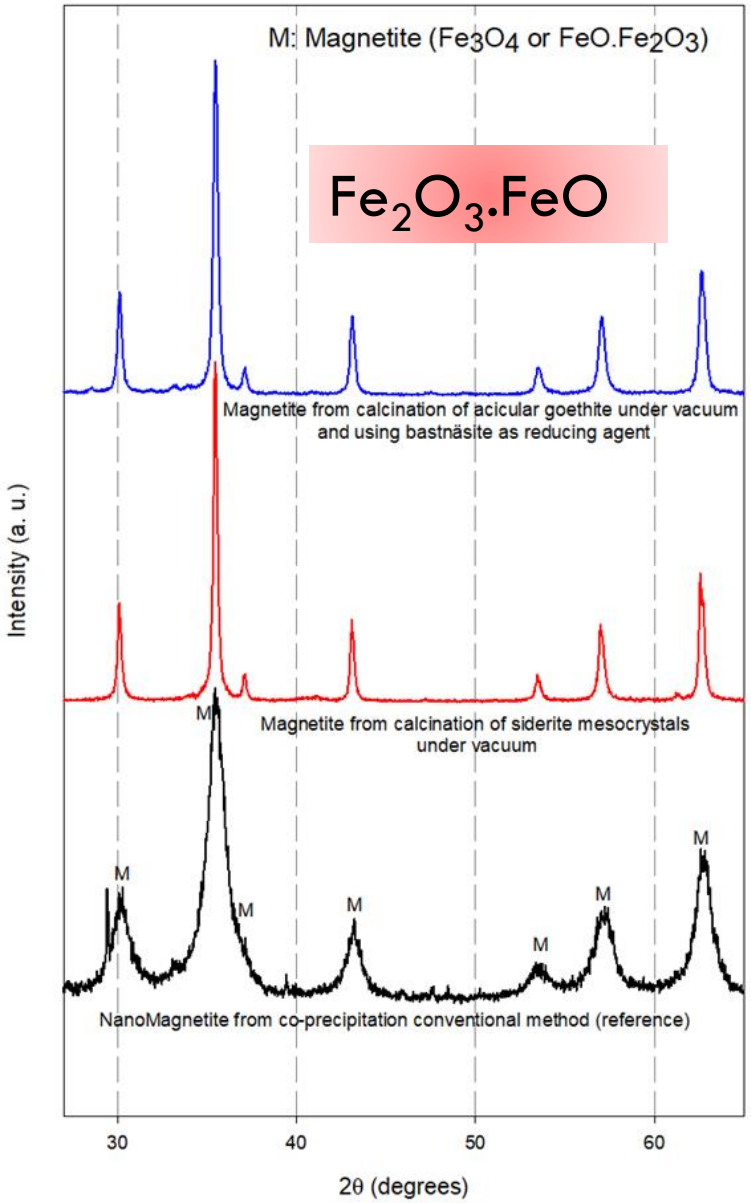

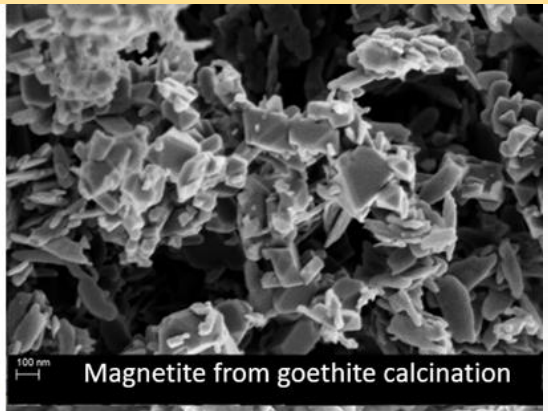

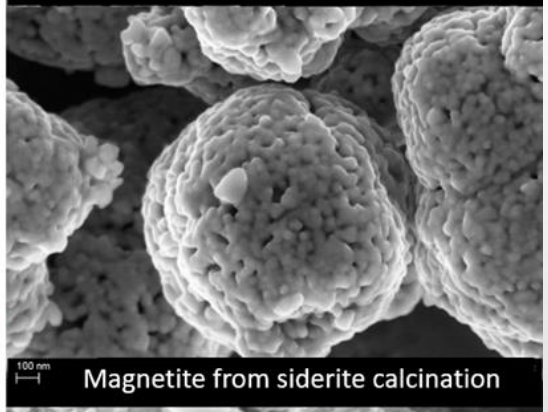

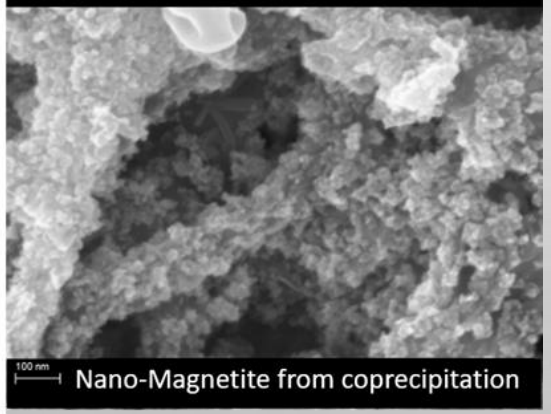

- G. Montes-Hernandez, R. Chiriac, N. Findling, F. Toche, F. Renard. Synthesis of Ceria (CeO2 and CeO2-x) Nanoparticles via Decarbonation and Ce(III) Oxydation of Synthetic Bastnäsite (CeCO3F). Materials Chemistry and Physics 172 (2016) 202-210.

- G. Montes-Hernandez. Synthesis of Magnetite, Ceria and Magnetite-Ceria Materials by Calcination of Nanostructured Precursor-Minerals. Materials Letters 276 (2020) 128246.

- G. Montes-Hernandez, P. Beck, F. Renard, E. Quirico, B. Lanson, R. Chiriac, N. Findling. Fast precipitation of acicular goethite from ferric hydroxide gel under moderate temperature (30 and 70 C degrees). Crystal Growth & Design 11 (2011) 2264-2272.

- G. Montes-Hernandez, N. Findling, F. Renard. Direct and Indirect Nucleation of Magnetite Nanoparticles from Solution Revealed by Time-Resolved Raman Spectroscopy. Crystal Growth & Design 21 (2021) 3500-3510.

Synthesis of magnetite-ceria composite by complex redox reactions during calcination

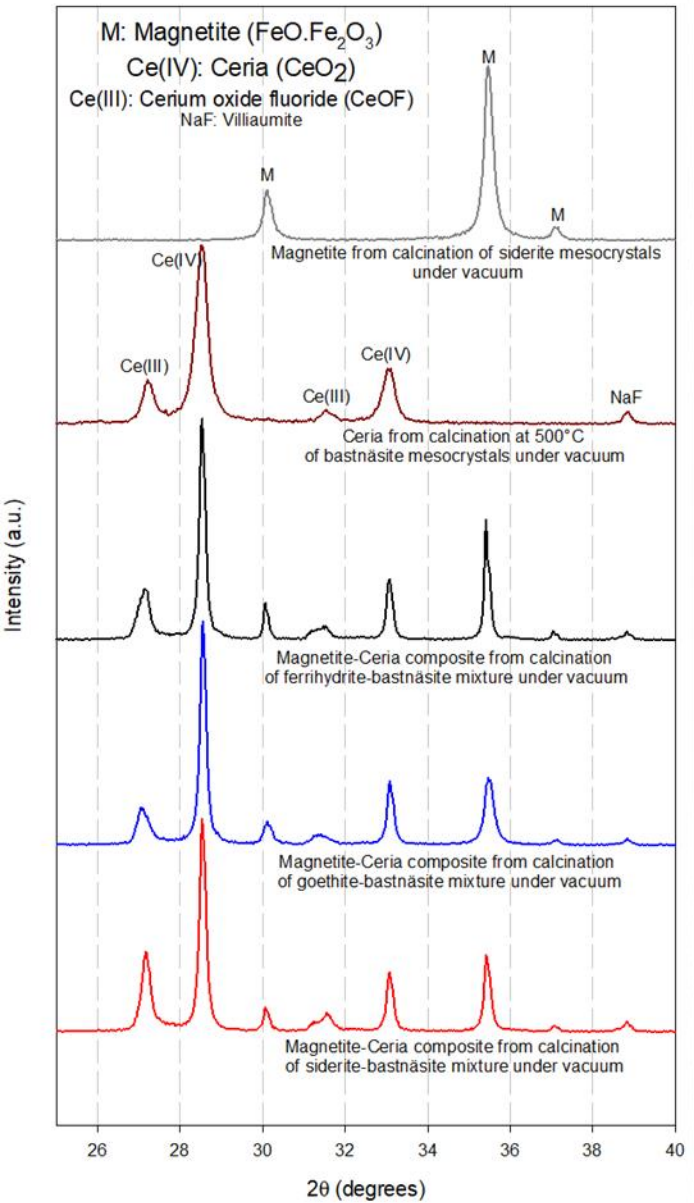

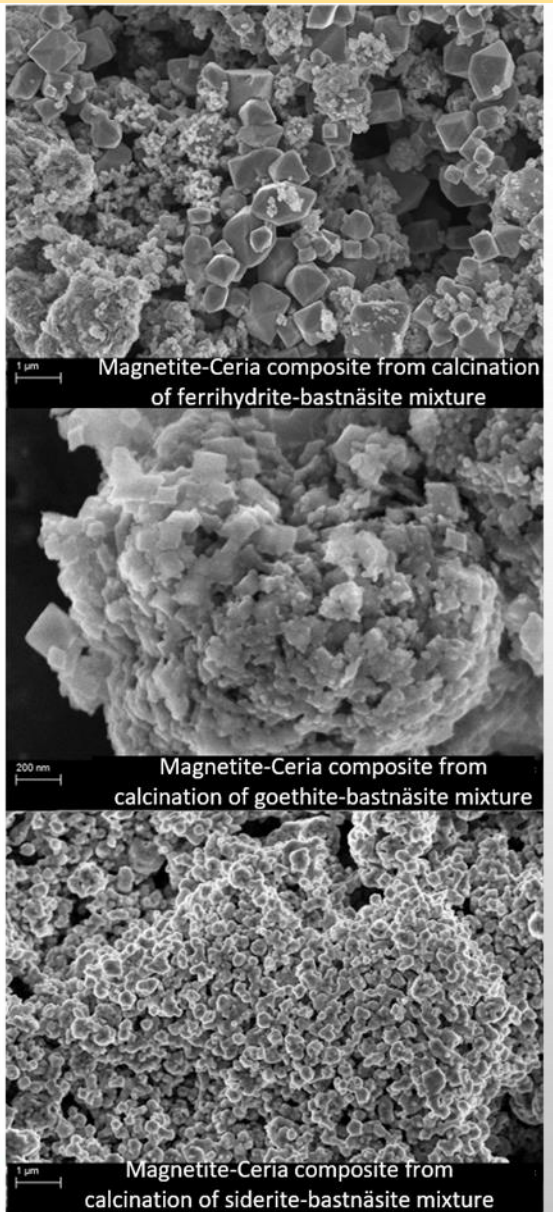

Fe_3O_4-CeO_2

- G. Montes-Hernandez, R. Chiriac, N. Findling, F. Toche, F. Renard. Synthesis of Ceria (CeO2 and CeO2-x) Nanoparticles via Decarbonation and Ce(III) Oxydation of Synthetic Bastnäsite (CeCO3F). Materials Chemistry and Physics 172 (2016) 202-210.

- G. Montes-Hernandez. Synthesis of Magnetite, Ceria and Magnetite-Ceria Materials by Calcination of Nanostructured Precursor-Minerals. Materials Letters 276 (2020) 128246.

Synthesis of tubular chrysotile under hydrothermal conditions

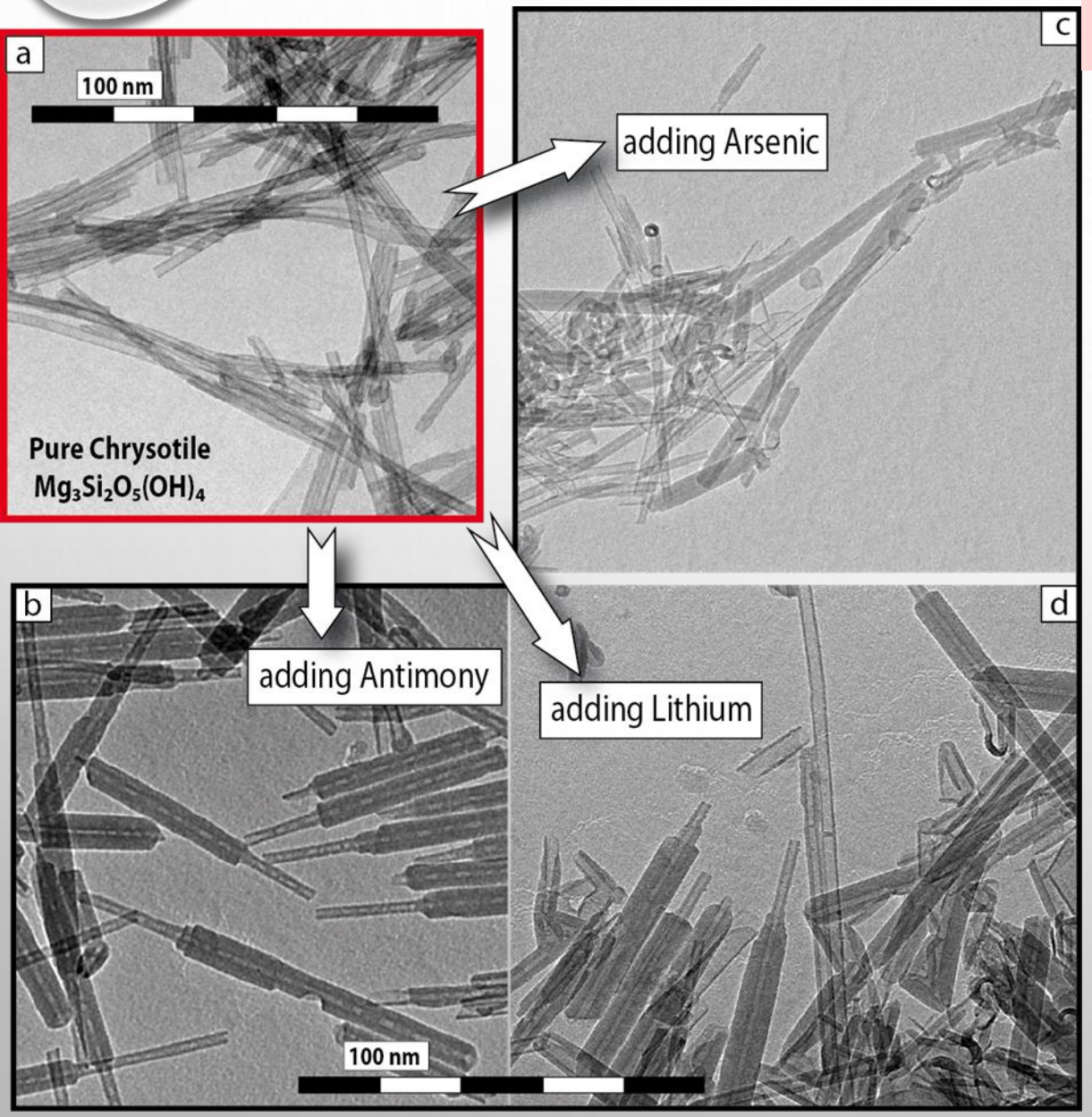

$Mg_3Si_2O_5(OH)_4$

- R. Lafay, G. Montes-Hernandez, E. Janots, R. Chiriac, N. Findling, F. Toche. Nucleation and growth of chrysotile nanotubes in H2SiO3-MgCl2-NaOH medium from 90 to 300°C, Chemistry – A European Journal 19 (2013) 5417-5424.
- R. Lafay, G. Montes-Hernandez, E. Janots, A-L. Auzende, R. Chiriac, D. Lemarchand, F. Toche. Influence of trace elements on the textural properties of synthetic chrysotile : Complementary insights from macroscopic to nanoscopic measurements, Microporous and Mesoporous Materials 183 (2014) 81-90.

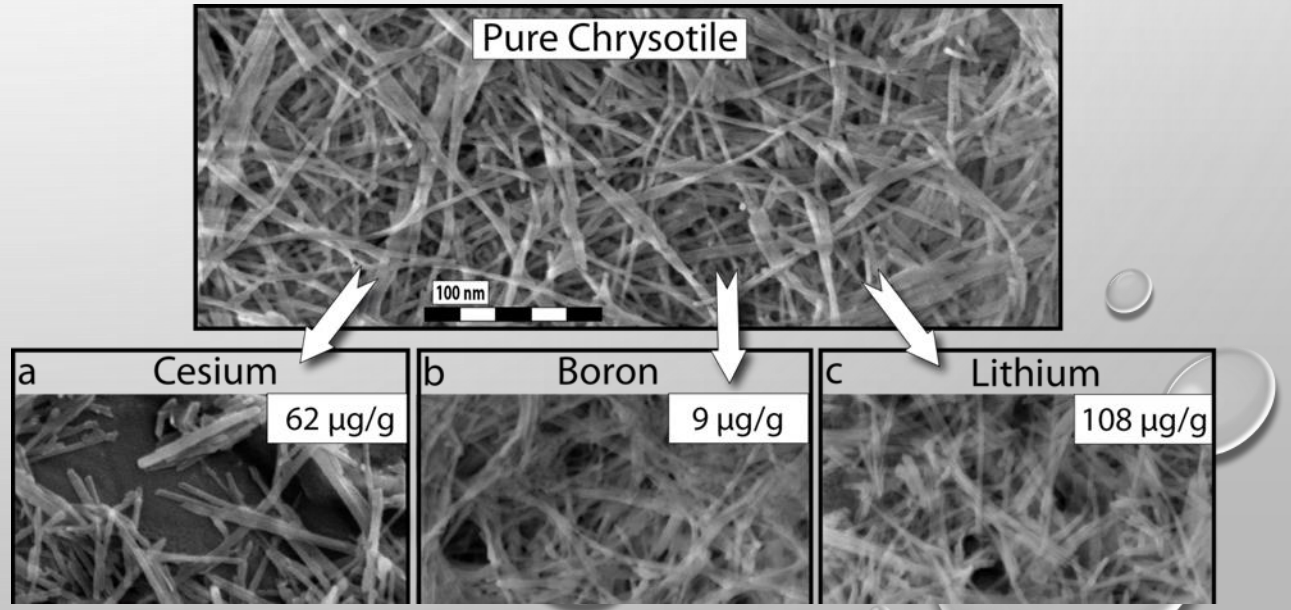

Ag Particles by simple reduction process at room T (confidential)

Ag^0 Crystals

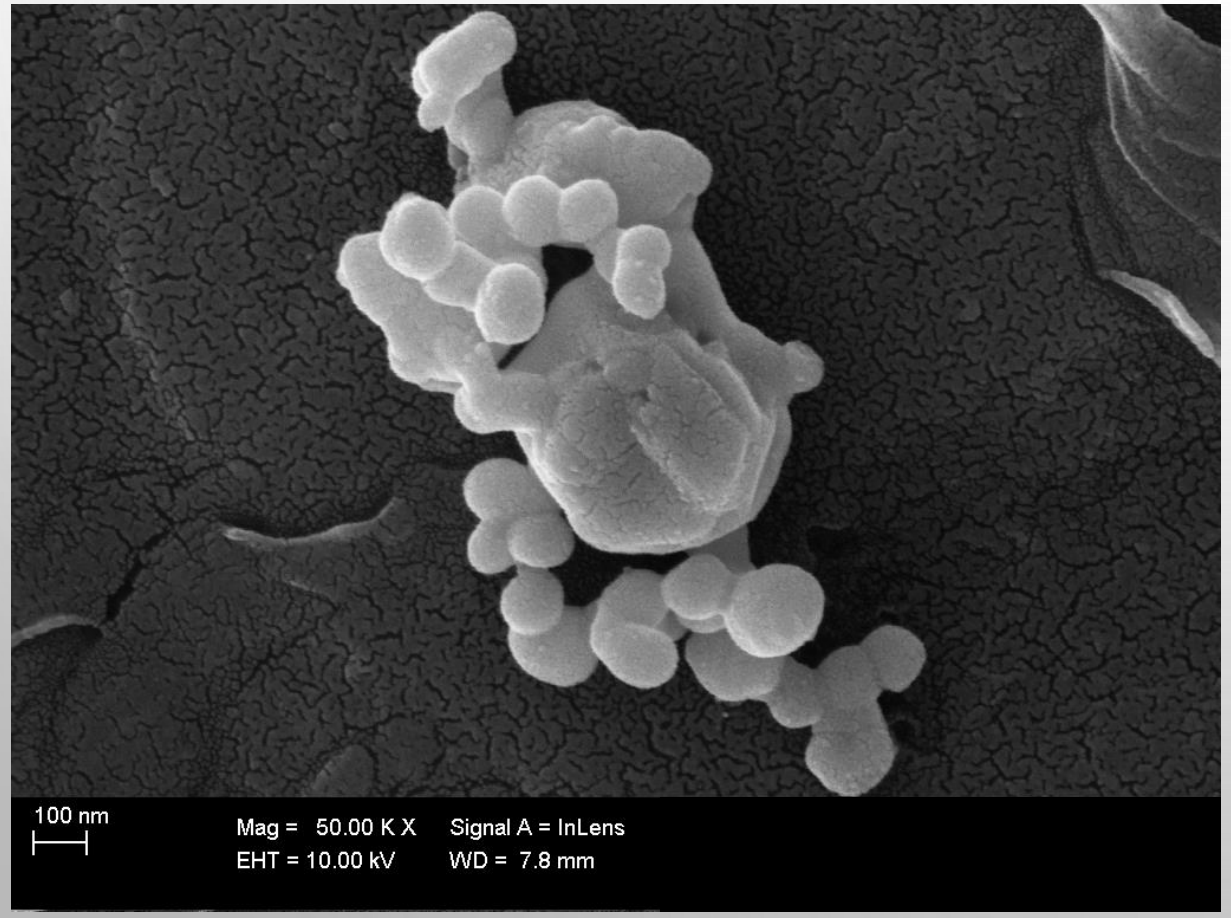

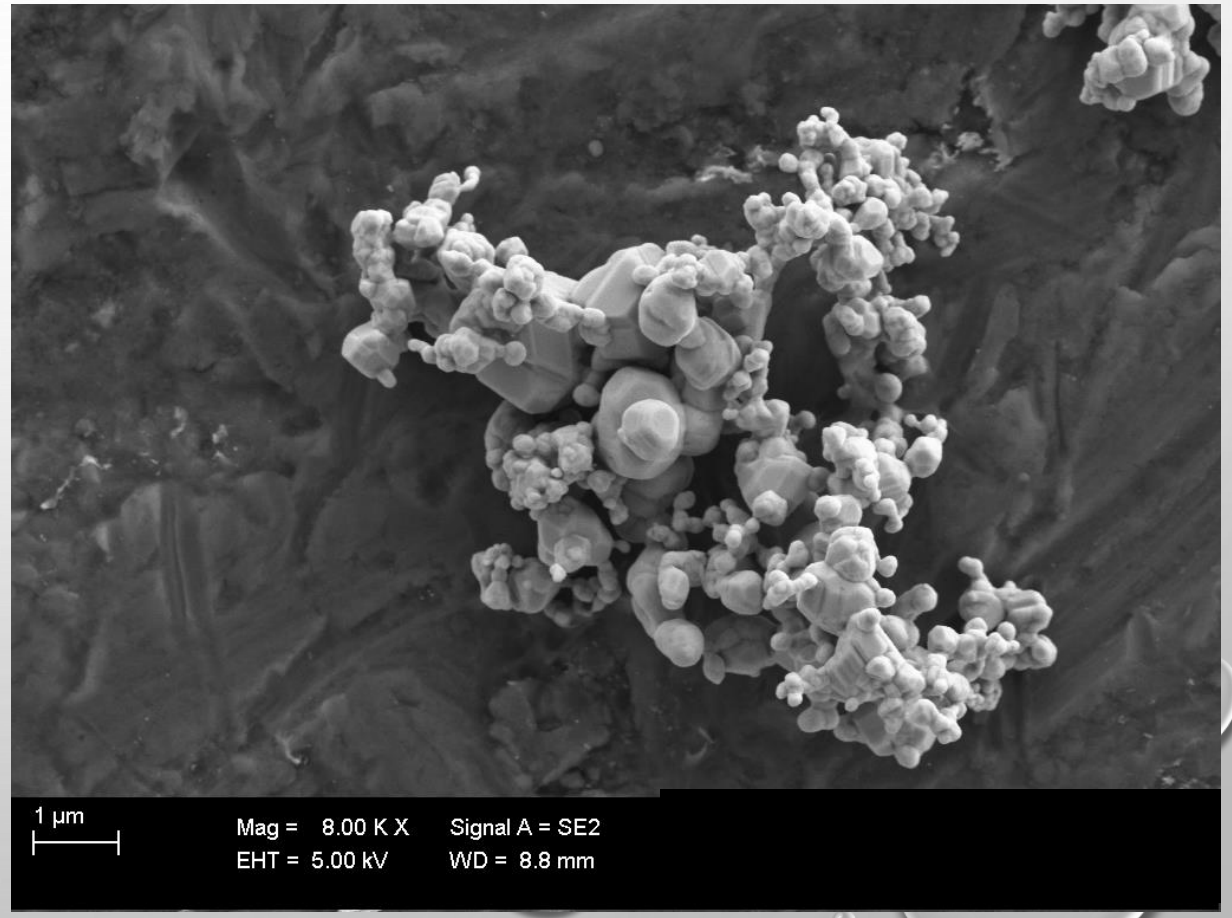

Ag Nanoparticles by simple reduction process in textile fibers

ISTerre

Ag^0 Nanocrystals

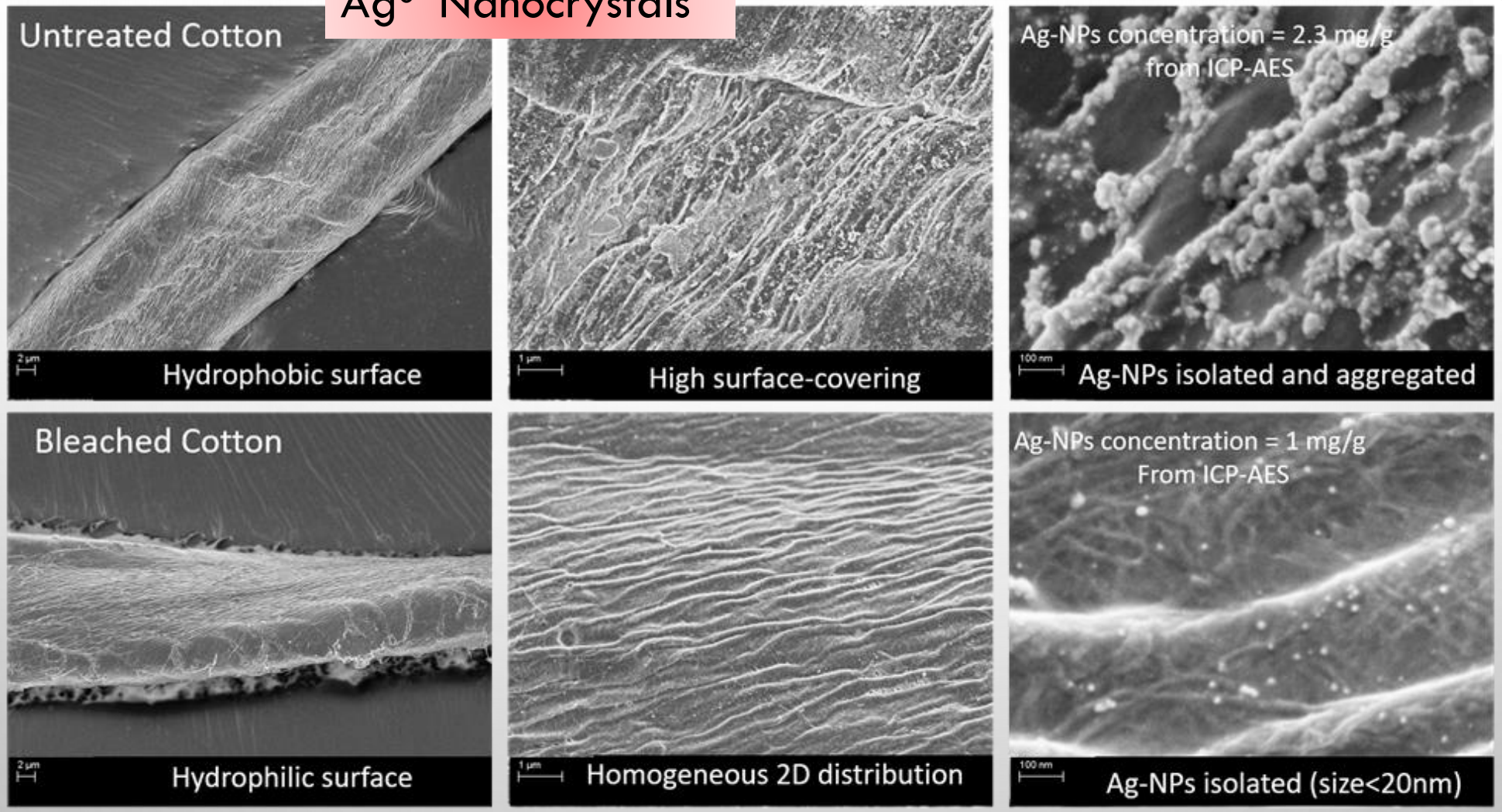

- G. Montes-Hernandez, M. Di Girolamo, G. Sarret, S. Bureau, A. Fernandez-Martinez, C. Lelong, E. Eymard Vernain. In situ Formation of Silver Nanoparticles (Ag-NPs) onto Textile Fibers. ACS Omega 6 (2021) 1316-1327.

Magnetite Nanoparticles and Microparticles by coprecipitation at room T and under hydrothermal conditions

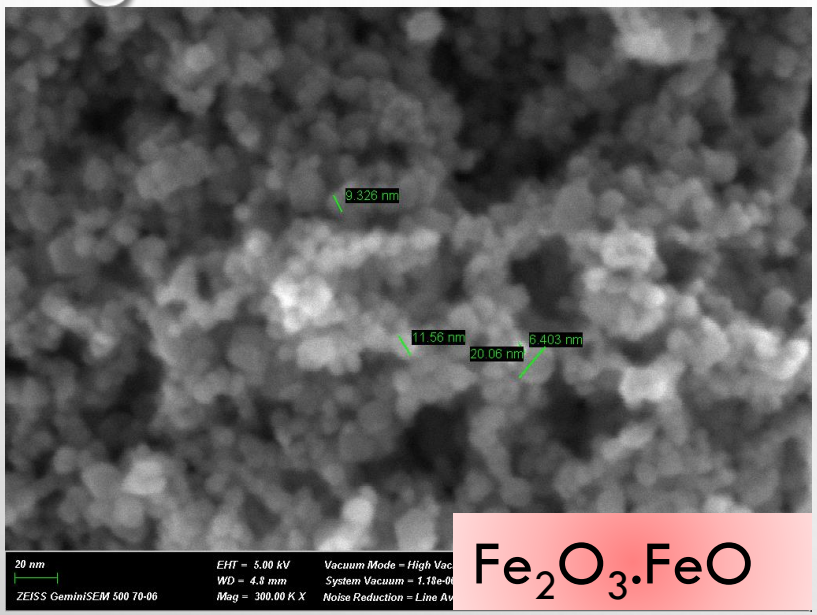

$Fe_2O_3.FeO$

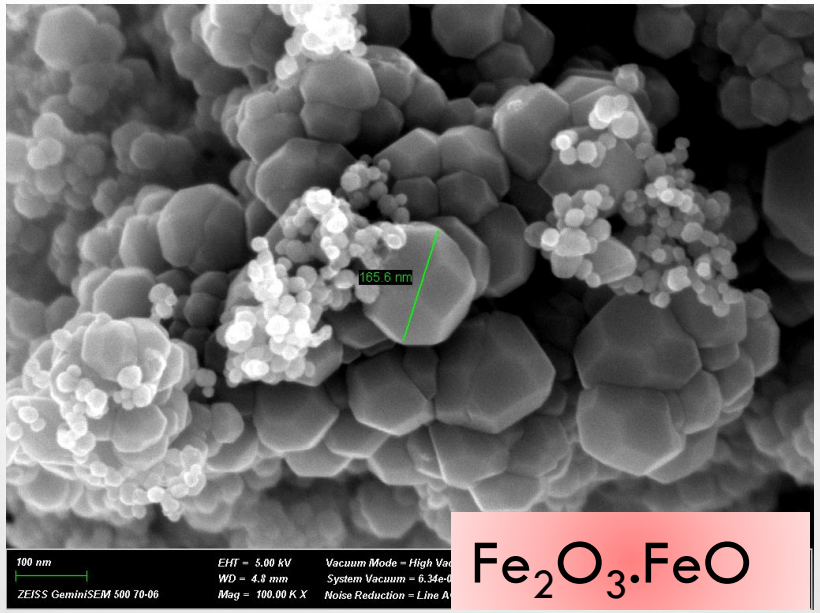

$Fe_2O_3.FeO$

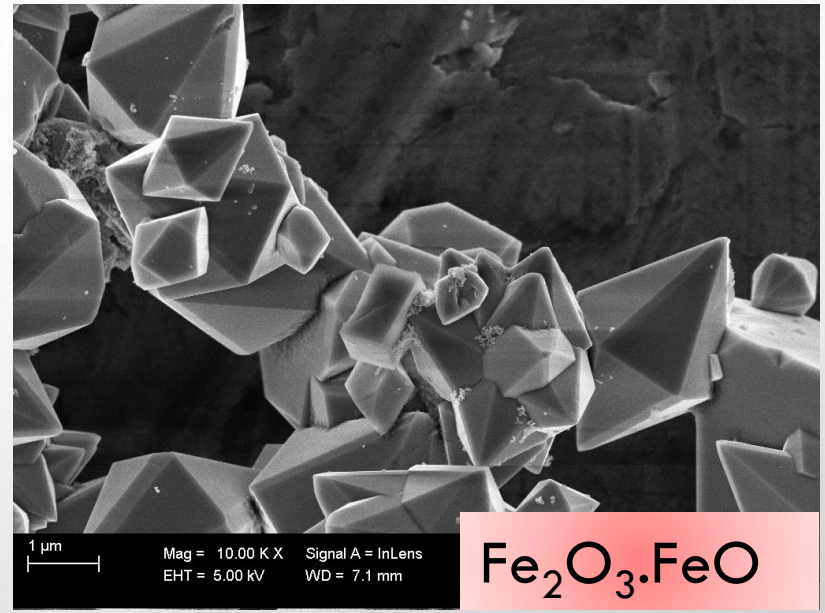

$Fe_2O_3.FeO$

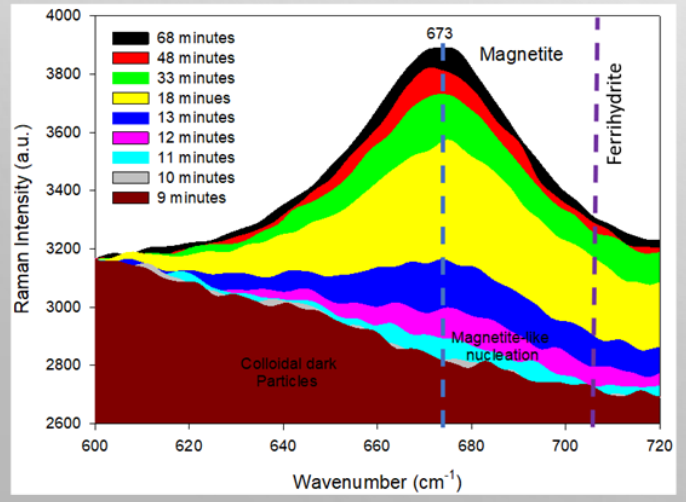

- G. Montes-Hernandez, N. Findling, F. Renard. Direct and Indirect Nucleation of Magnetite Nanoparticles from Solution Revealed by Time-Resolved Raman Spectroscopy. Crystal Growth & Design 21 (2021) 3500-3510.

Synthesis of siderite-magnetite composite under hydrothermal conditions (confidential)

$FeCO_3$-Fe_3O_4

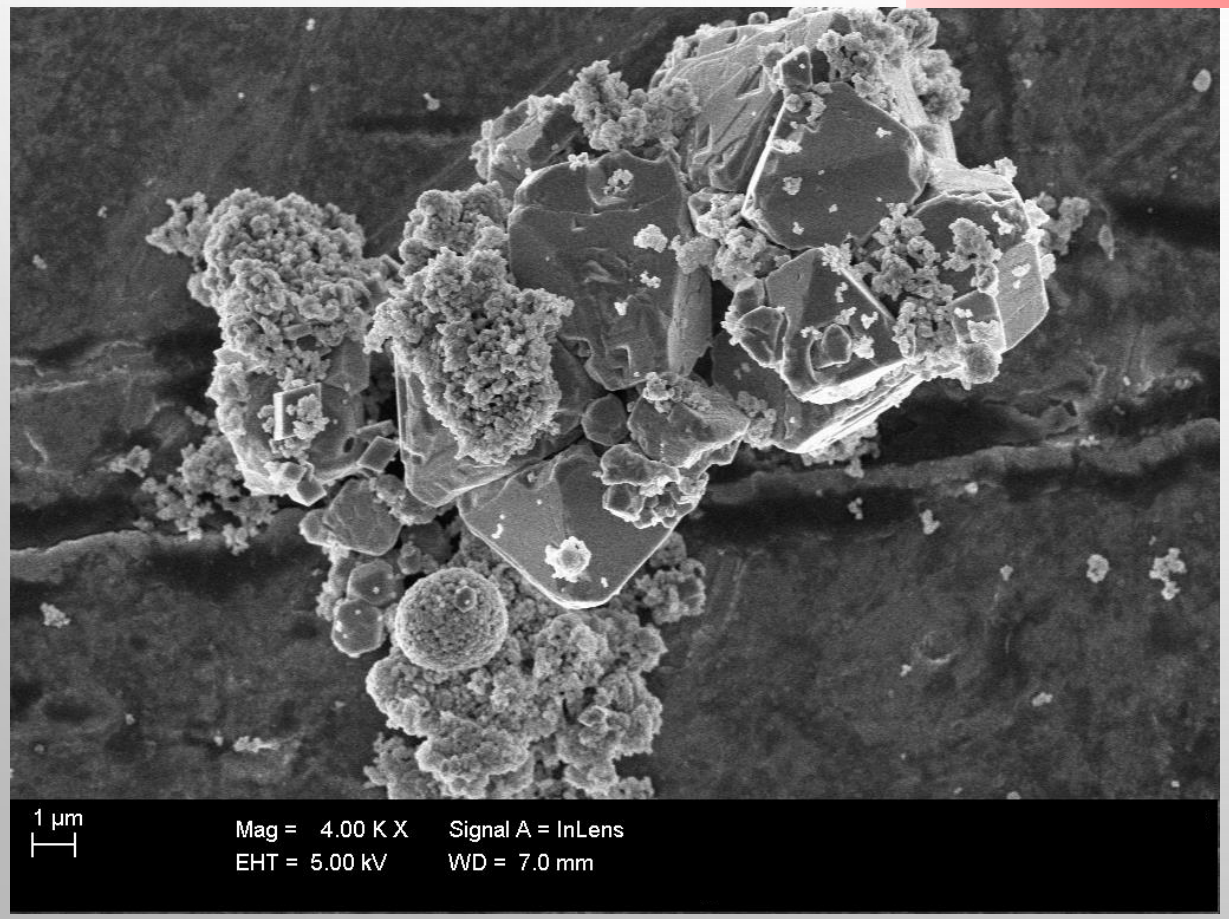

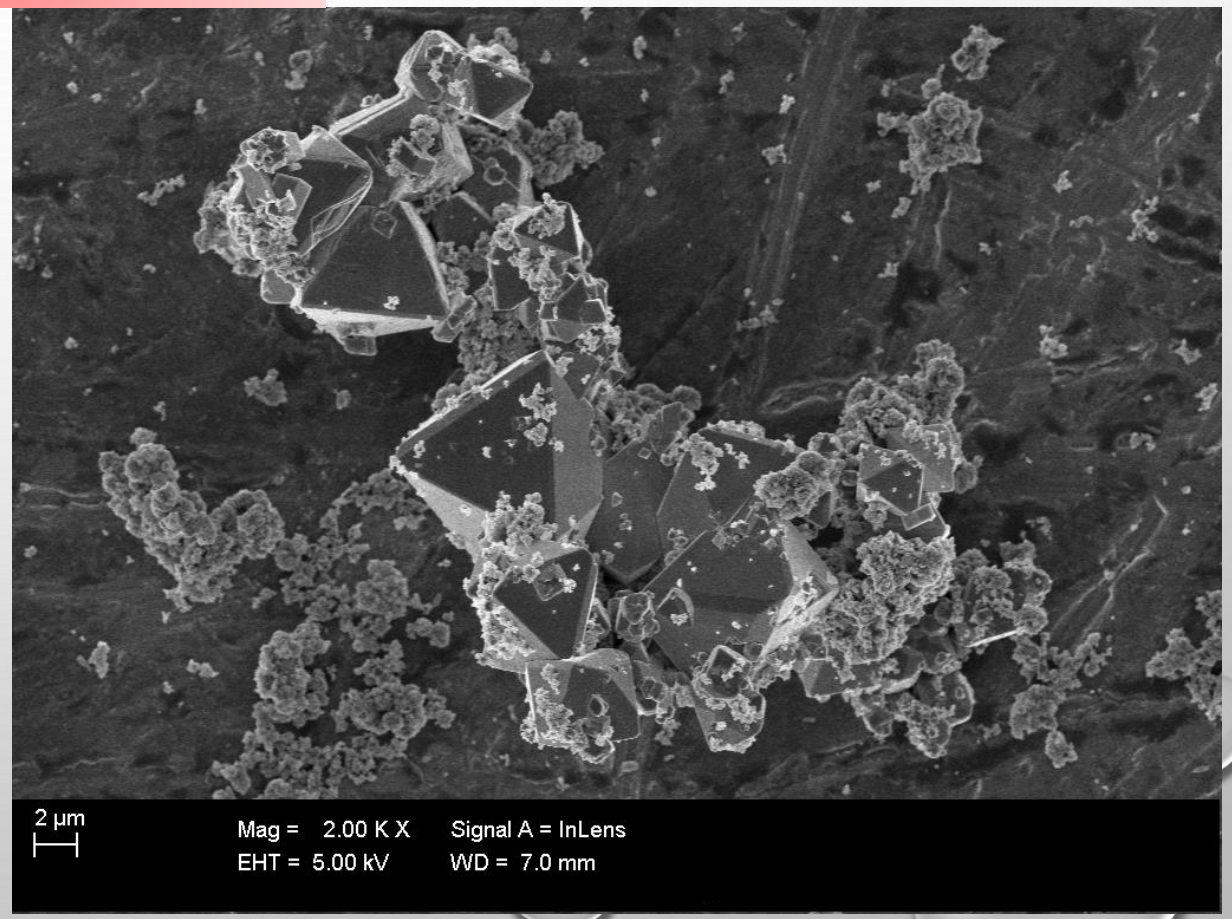

Synthesis of Struvite and Newberyite at room T (confidential)

ISTerre

$NH_4MgPO_4 \cdot 6\ H_2O$

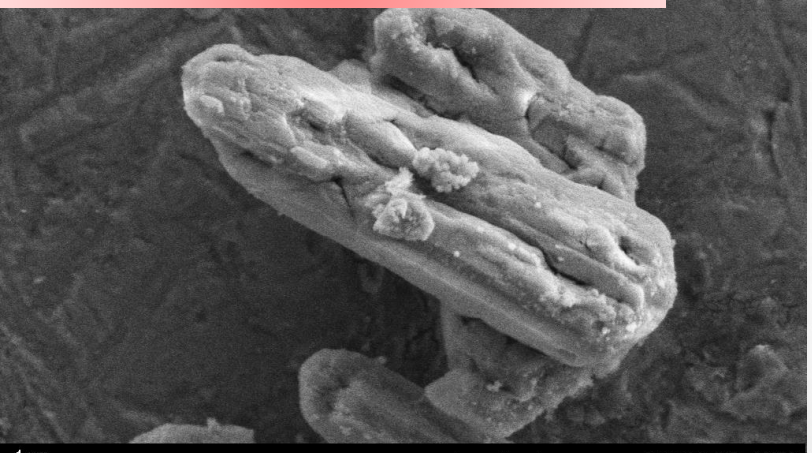

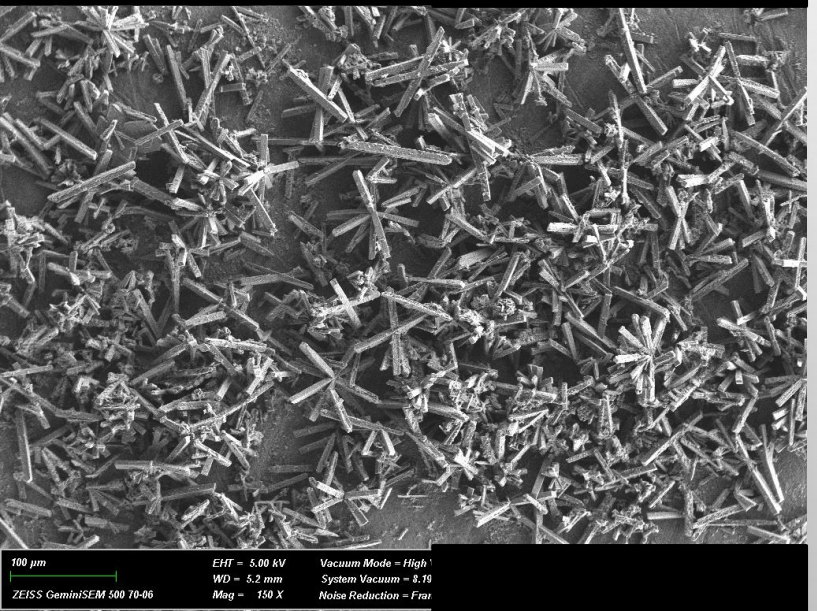

$MgHPO_4 \cdot 3\ H_2O$

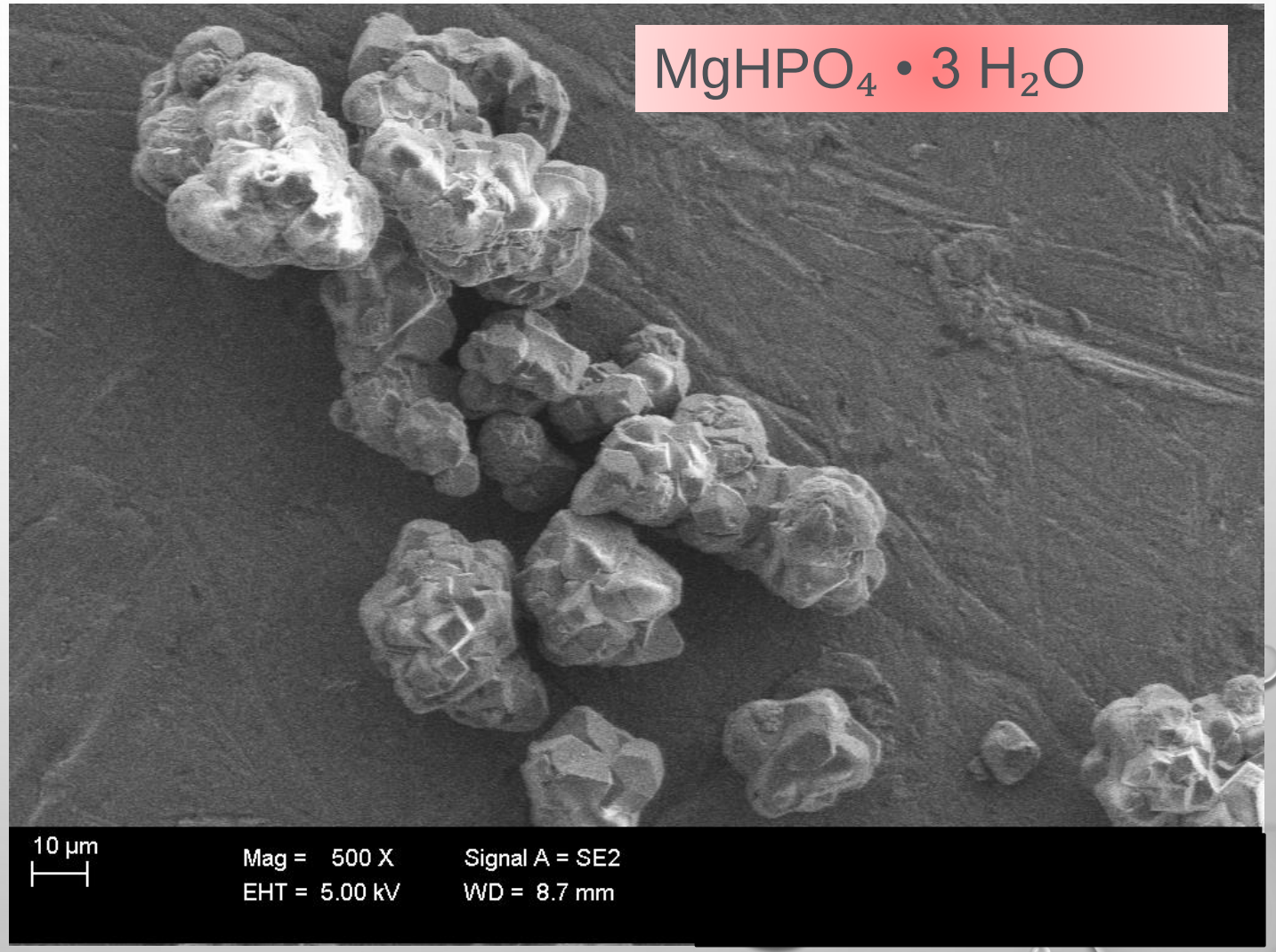

Synthesis of calcium oxalate at room T (confidential)

CaC_2O_4

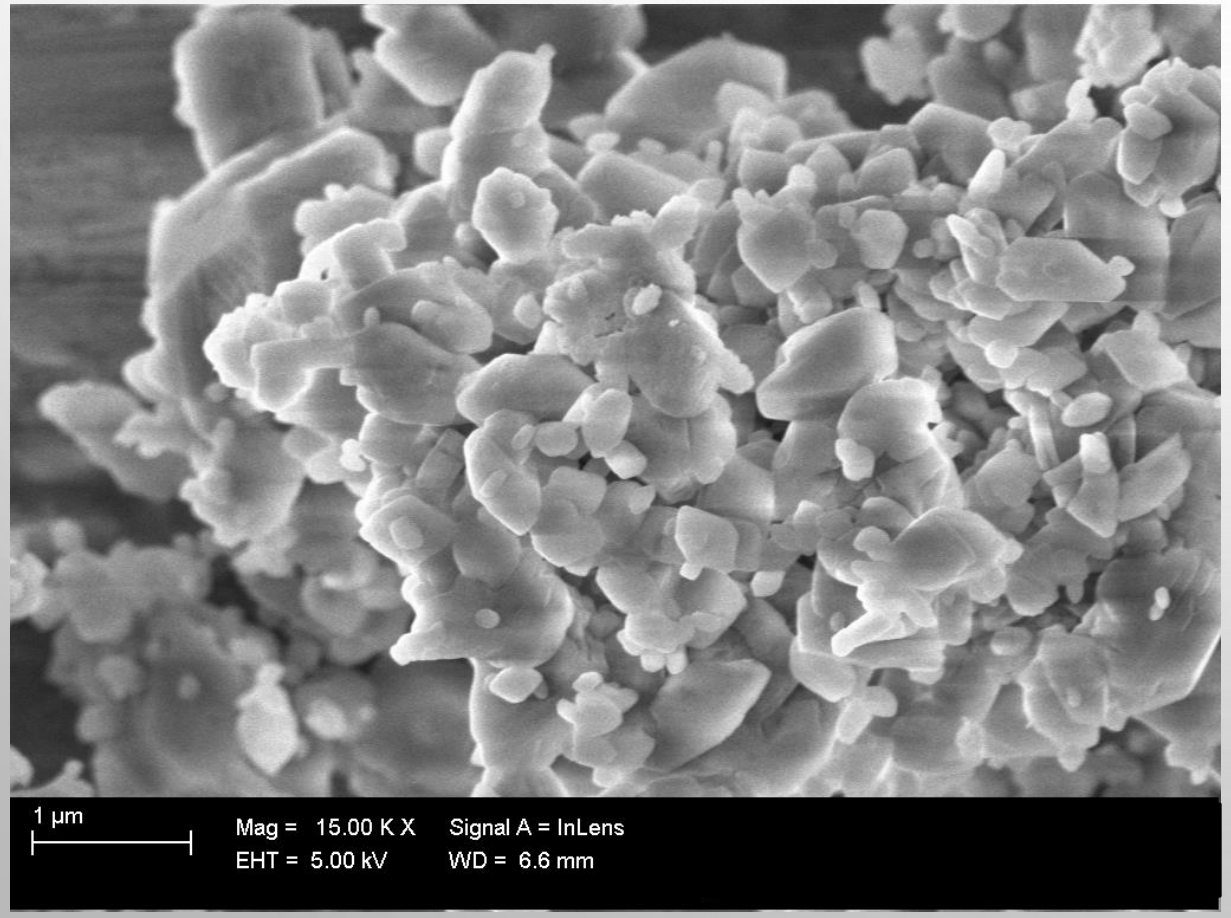

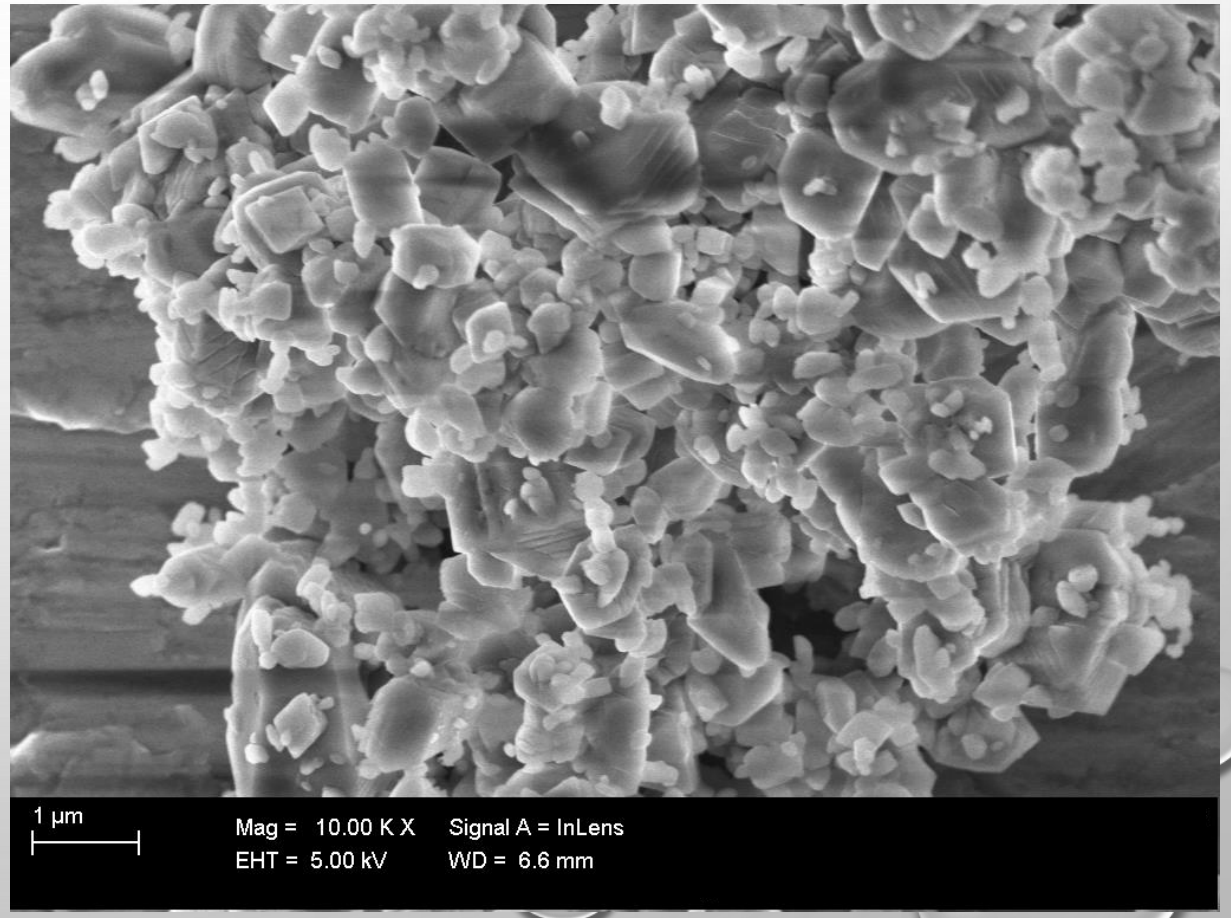

Synthesis of vaterite mesocrystals at room T (confidential)

$CaCO_3$

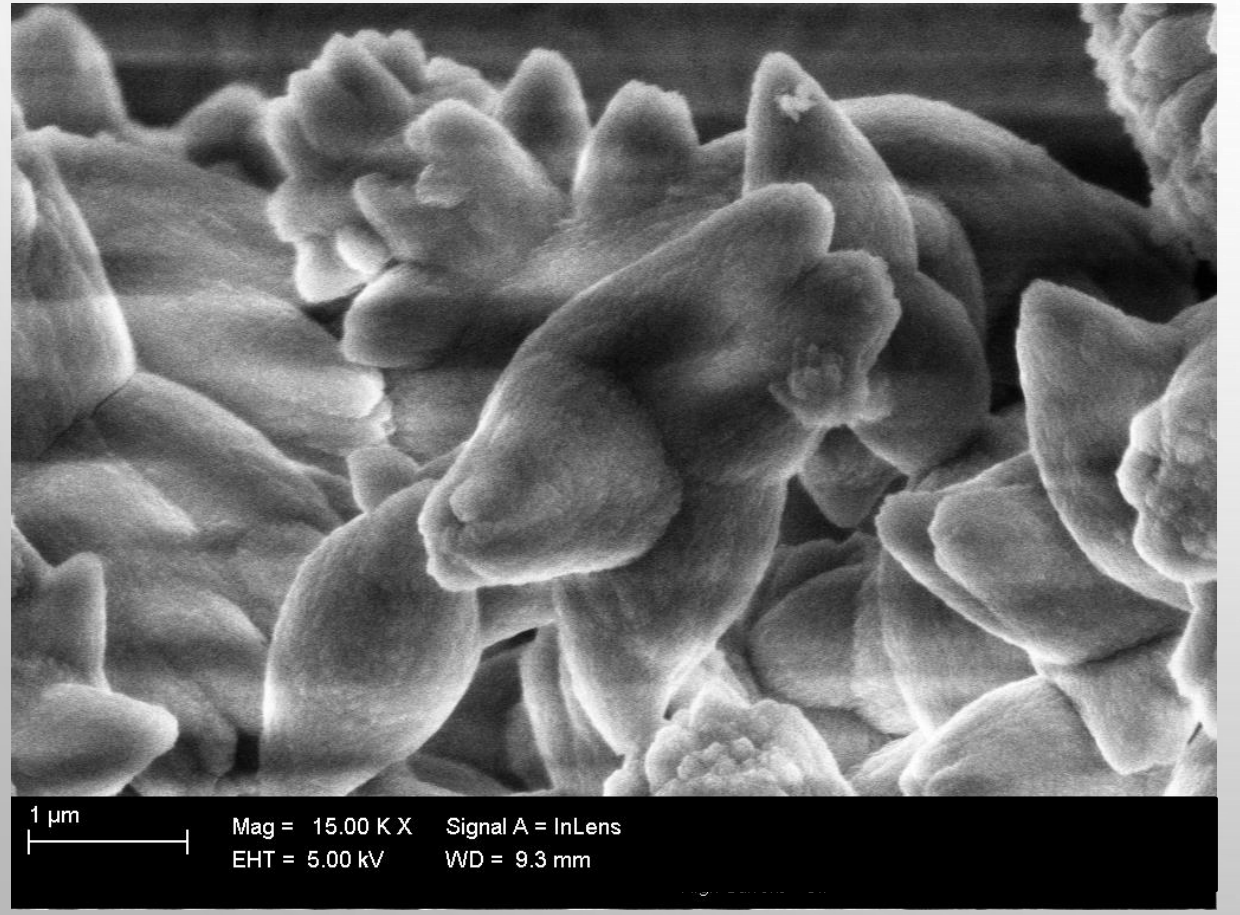

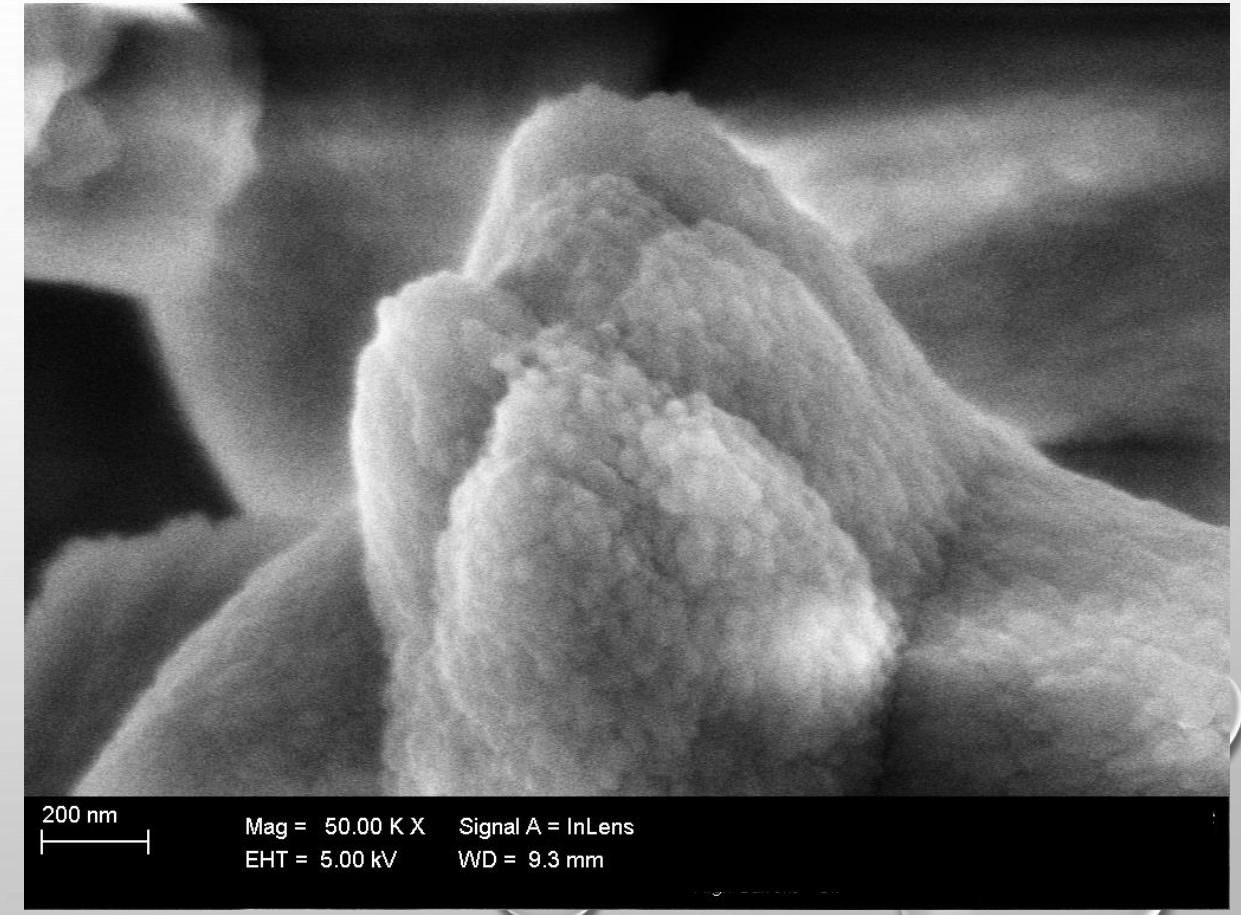

Synthesis of Mg-clay by glass alteration in Mg-carbonate media under mild conditions (confidential)

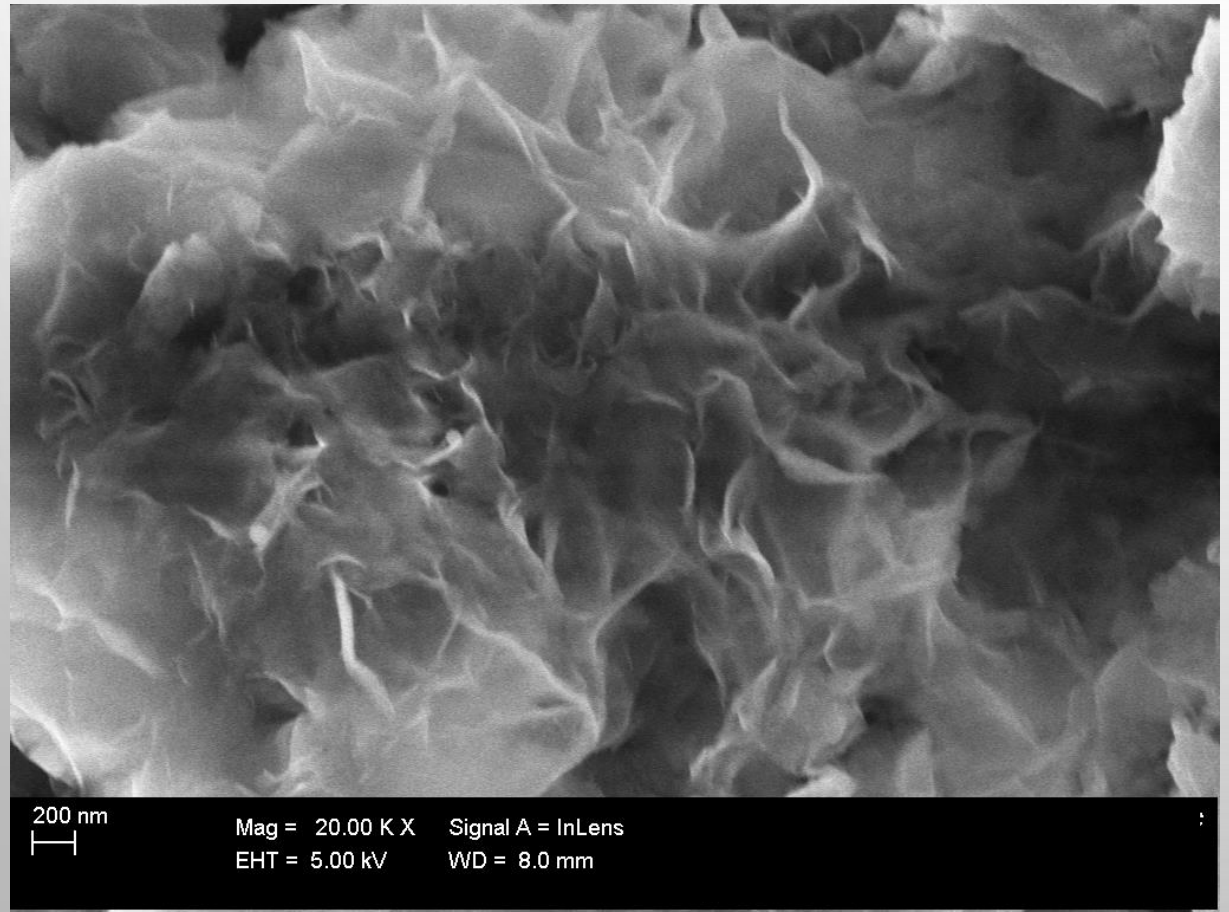

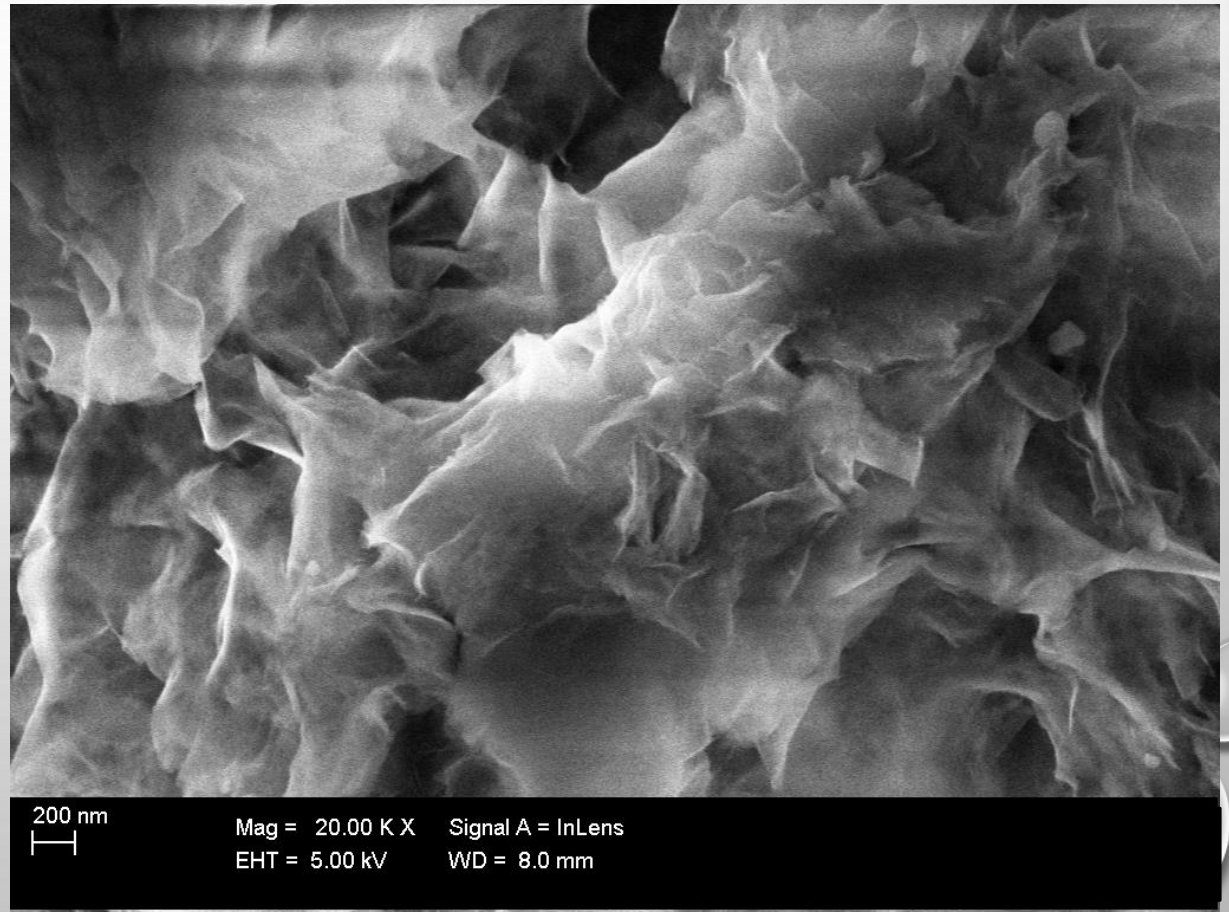

Synthesis of xonotlite by a hydrothermal method (confidential)

$Ca_6Si_6O_{17}(OH)_2$

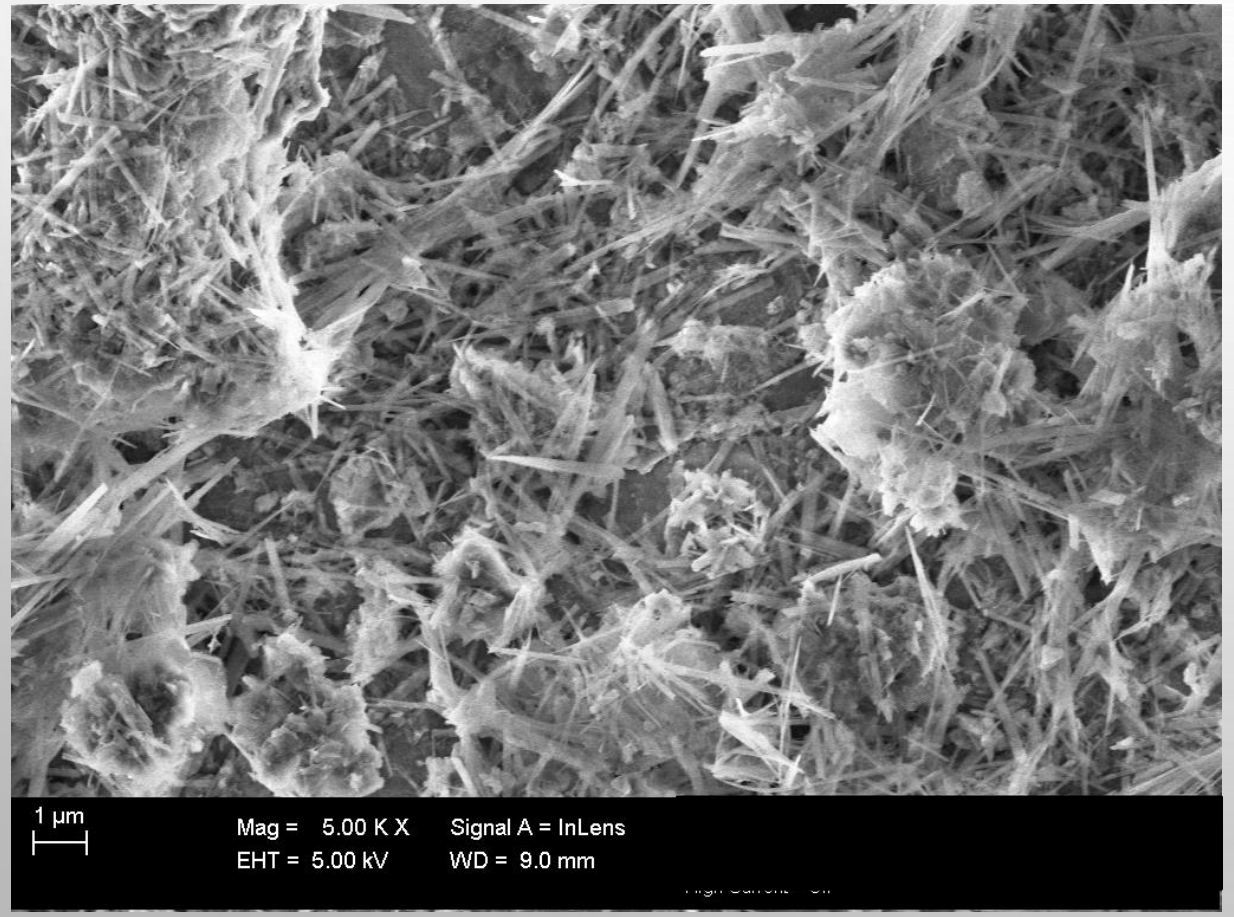

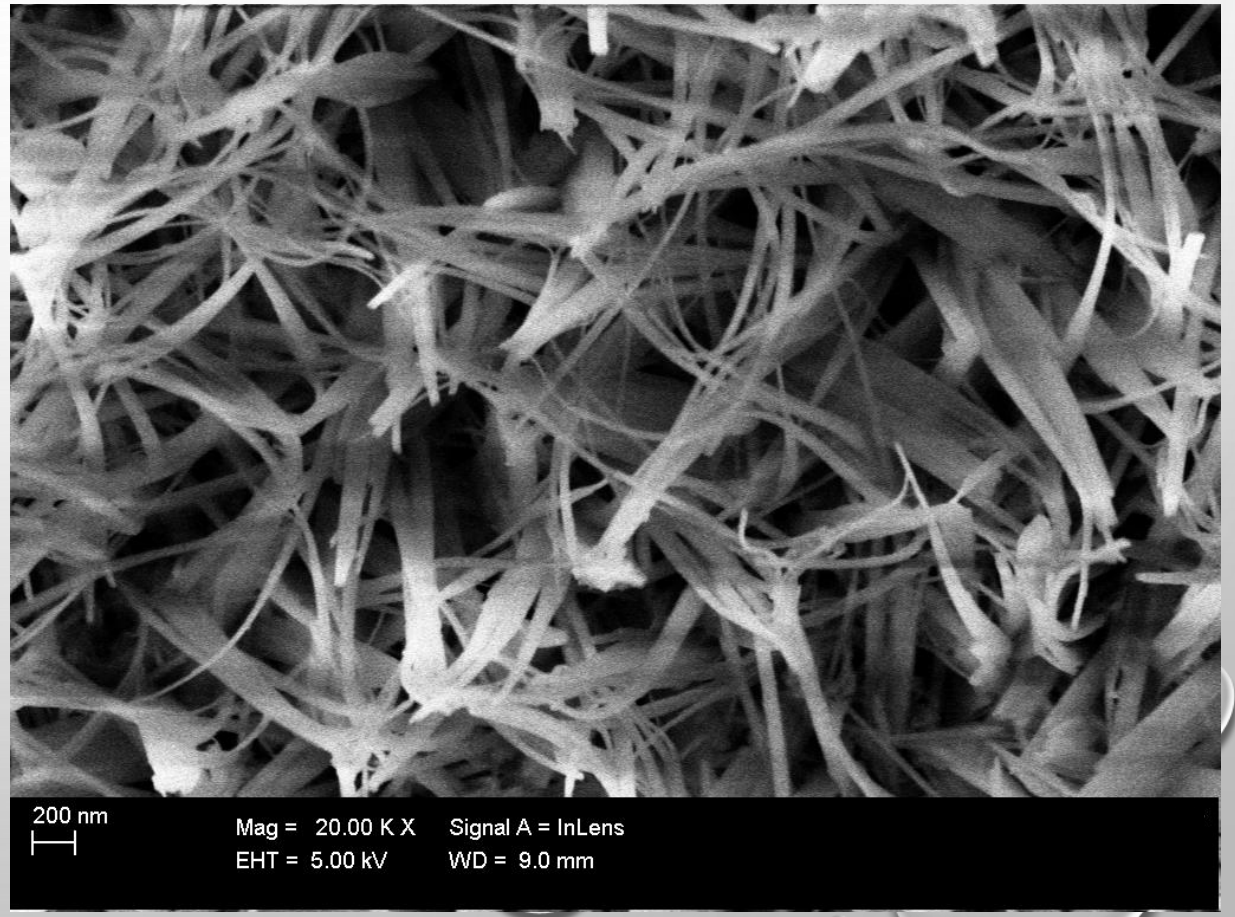

Au Nanoparticles by simple reduction process at room T (confidential)

Au^0 Nanocrystals